COMPOSITION MEASUREMENTS OF THE TOPSIDE IONOSPHERE USING A MAGNETIC MASS SPECTROMETER

Ion Mass Spectrometer on ISIS-II Spacecraft

J. H. Hoffman
University of Texas at Dallas
P. O. Box 688
Richardson, Texas 75080

January 20, 1975
Final Report

Prepared for
GODDARD SPACE FLIGHT CENTER
Greenbelt, Maryland 20771

PREFACE

The ion mass spectrometer (IMS) on the ISIS-II satellite measures the composition and distribution of positive ions in Earth's ionosphere in the mass range of 1 to 64 atomic mass units. Launched on 1 April 1971 the satellite is in a near circular orbit of 1358 km perigee, 1428 km apogee and 88.1° inclination. Successful operation of the ion mass spectrometer has continued from turn-on to date, a period of nearly four years. Significant data have been received which show a wide variation in ion composition at night near the equator and in the daytime poleward of the plasmapause. These data have enabled further study of the polar wind which was verified by a similar instrument on the Explorer 31 satellite. Additionally, the experiment produced timely data during the August, 1972 magnetic storm to show the development of a unique ionosphere above the plasmapause during the period of the storm.

This final report documents the scientific objectives and results of the experiment, the technical description of the instrument and presents a bibliography with sample papers attached and a summary of recommendations for further study.

TABLE OF CONTENTS

1.0 SCIENTIFIC OBJECTIVES

1.1 GENERAL

This experiment called the Ion Mass Spectrometer (IMS) was designed to study the positive ion composition of the Earth's ionosphere through measuring the concentrations of each ion species with a small magnetic mass spectrometer operating in two mass ranges: 1 - 8 and 8 - 64 atomic mass units (amu). The instrument was carried on board the ISIS-II spacecraft. It has mapped the distribution of each positive ion constituent in the ionosphere at a nearly constant altitude of 1400 km for almost four years, since the ISIS-II satellite launch on April 1, 1971.

Magnetic deflection mass spectrometers have been used since 1964 to study the composition of the ionosphere from rockets and satellites. Such instruments have been successfully flown on a number of high altitude rockets and two satellites, Explorer 31 and Explorer 51, besides ISIS-II. The experiment covered by this report enabled a continuation of Explorer 31 ionospheric studies extended to the period of time near the solar maximum. While the Explorer 31 instrument covered the range of 1 - 20 amu, the ISIS-II instrument had an extended mass range to 64 amu.

The data are frequently plotted as a function of dip latitude as shown in Figure 1. Other ephemeris data and time are shown at the bottom of the plot. This is an example of a daytime (late afternoon) ionosphere showing both winter in the southern hemisphere and summer in the north at the essentially constant satellite altitude of 1400 km. The constancy of the ISIS-II orbit is a great advantage in presenting such data because latitudinal and local time variations can be studied without the usual complications introduced by simultaneous altitude changes. In this case, the satellite is in sunlight, but at -45° dip latitude the satellite

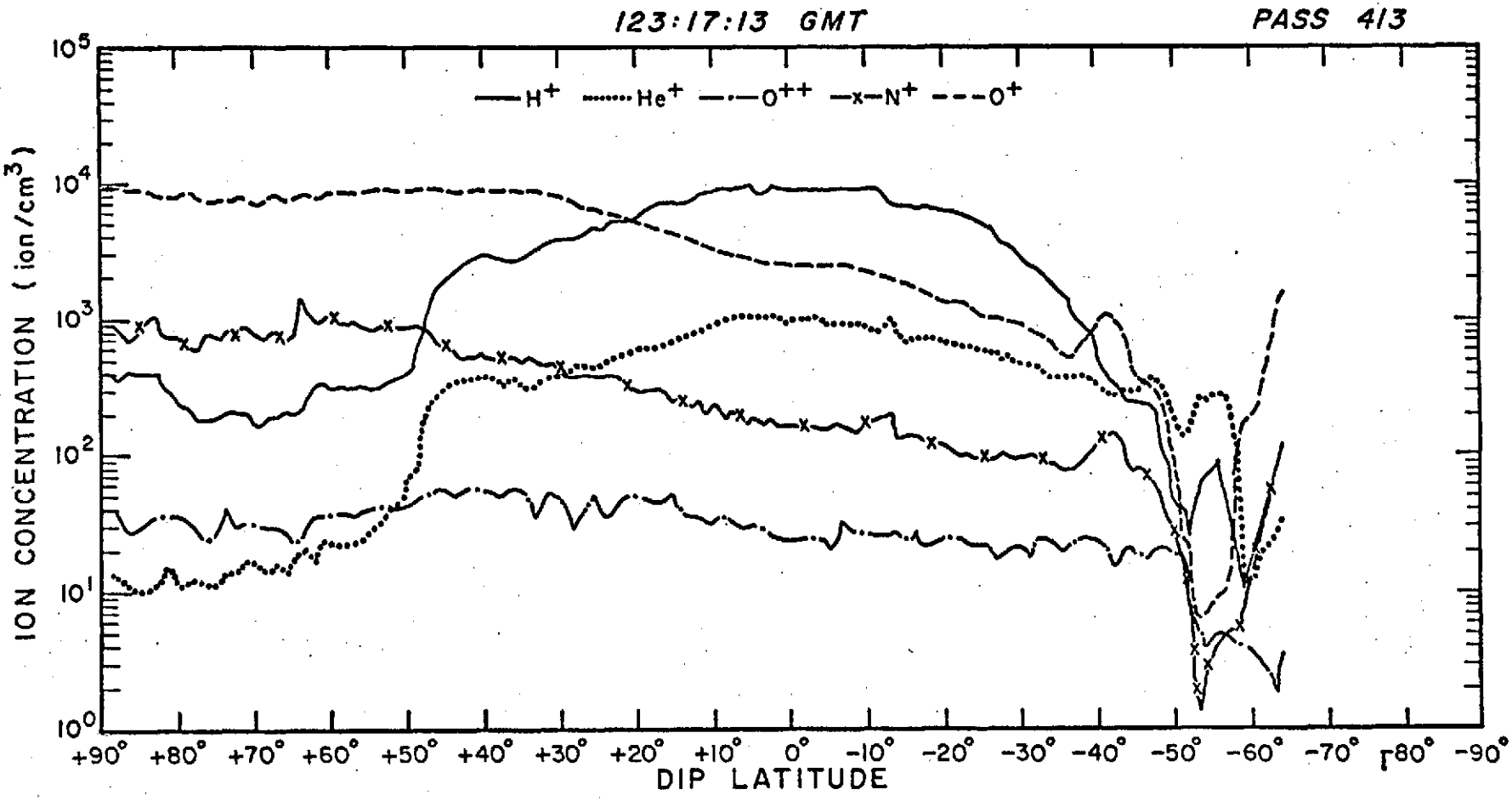

Figure 1

Pole-to-pole plot of ion daytime concentrations. Northern summer is to the left; southern winter to the right. Local time is 1713 to 1810. Satellite altitude is essentially constant at 1400 km. At about -45° latitude the solar zenith angle exceeds 90°, but the orbit altitude is still sunlit.

crosses the terminator passing into a region where a part of the ionosphere below the spacecraft is in darkness. O^+ is the dominant species in the summer day above $+20^\circ$ dip latitude, and its concentration remains very flat all the way to the pole showing no evidence of a high latitude trough. The H^+, while dominant at the equator, decreases gradually until 45°N where a steep negative gradient, indicative of the plasmapause, is observed. It then remains fairly flat out to the pole at a level a factor of 30 to 40 below the O^+. He^+ tends to follow H^+ at about 1 order of magnitude lower, showing the plasmapause gradient and equatorial bulge. The behavior of O^+ and He^+ in the equatorial to midlatitude region is longitude dependent, as is discussed by Breig and Hoffman (1975). In Figure 1, the absence of an equatorial trough is typical of the $+90^\circ$ longitude case discussed in the reference.

In the southern hemisphere, H^+ is the dominant ion from the equatorial maximum to -40° where O^+ exhibits a small enhancement centered about -42°. He^+ tends to follow H^+ until -30°, where its rate of decrease is less, resulting in He^+ becoming the dominant ion species between -50° and -58°, albeit, at a concentration of less than 300 cm^{-3}. (The He^+ region is not always present.) The sharp trough at -50° in all ion species is coincident with an upward flow of H^+ of 2 km sec^{-1} (polar wind) although the flux at this point is very low due to the low H^+ concentration. Farther poleward, O^+ again becomes the dominant species.

The details of the winter polar region are shown in Figure 2. The left hand side of the plot is an extension of Figure 1 showing the O^+ peak at -42°, the region of He^+ dominance and the O^+ peak at -66°. This peak is a consequence of the polar wind which establishes a parallel electric field along open magnetic field lines that increases the scale height of the ionosphere. The light ions have been largely depleted by

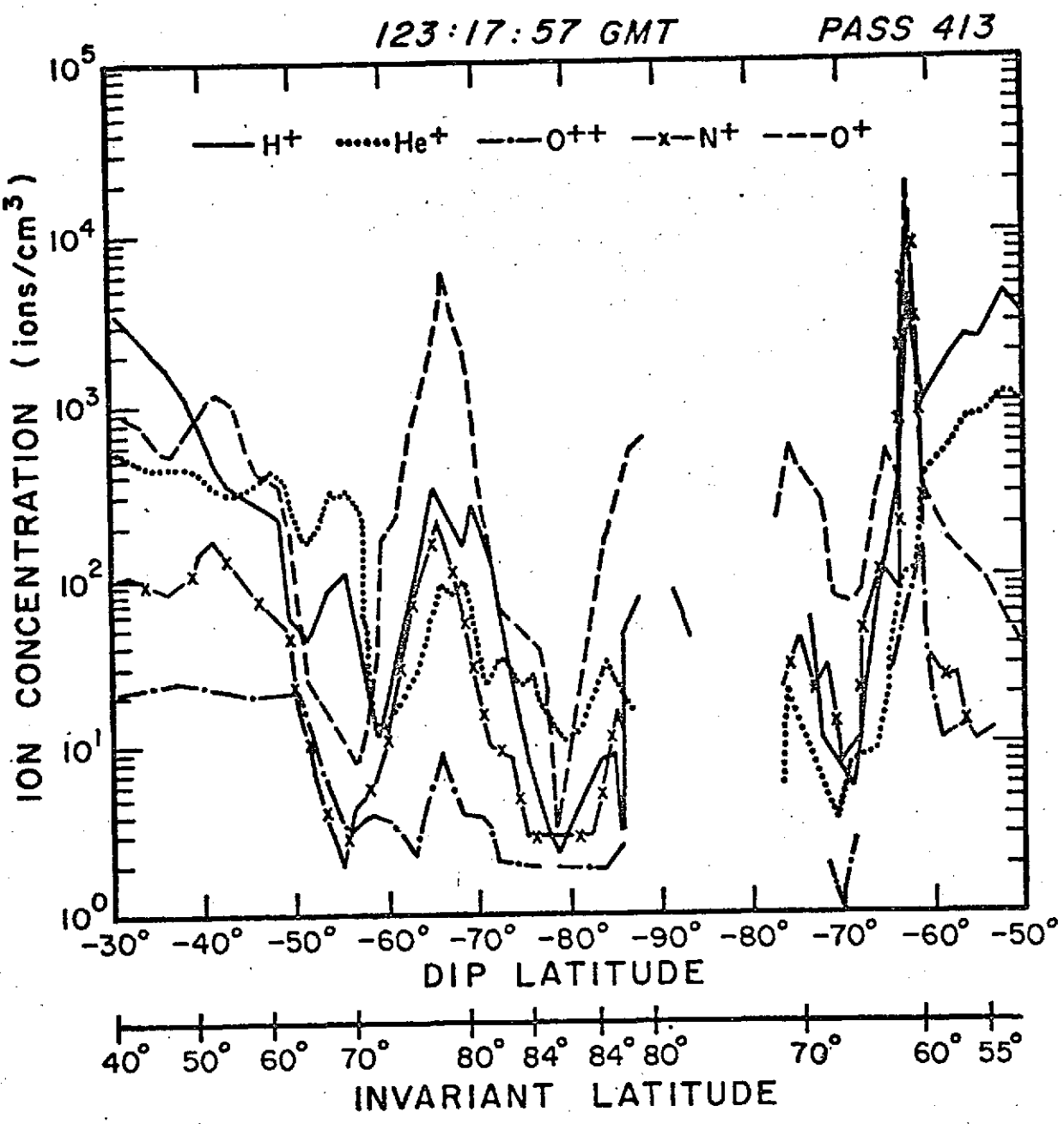

Figure 2.

Polar region of winter ionosphere at 1400 km. To the left is daytime an extension of Figure 4 (0400 LT); to the right nighttime (0400 LT). Large O^+ peak at -62° (night) identifies region of polar wind activity.

the flow leaving O^+ as the dominant species. The winter polar cap region is generally characterized by a very low ionic concentration as it is in darkness and no source of ionization is present there. Towards the night side, the pattern is essentially repeated except that the O^+ concentration becomes very low toward midlatitude due to the lower nighttime ion temperature.

Figure 3, a nighttime (0500) pole-to-pole pass a few days earlier than Figures 1 and 2, shows H^+ to be the dominant constituent between $\pm 45^o$. A steep gradient in H^+, indicative of the plasmapause, occurs at $\pm 50^o$, followed by a trough with O^+ dominance poleward, fairly flat in the summer, but with considerable structure in the winter (Figure 2). These are again the regions of polar wind flow. H^+ concentrations are down by a factor of 100 above the plasmapauses. He^+ exhibits a marked dip at the equator, with midlatitude peaks just equatorward of the plasmapause and a very steep gradient at the plasmapause. Farther poleward, the concentration is less than 10 ions cm^{-3}. However, the He^+ behavior is quite longitude dependent (Breig and Hoffman, 1975) with the equatorial dip especially pronounced near 0^o, the longitude of the data in Figure 3. O^+ appears to be anti-correlated with He^+ at the equator and midlatitudes, and exhibits a steep positive gradient at the light ion plasmapause before becoming the dominant species toward the poles. The polar cavity which exists in the winter, appears to be filled with principally O^+ ions is summer.

Taylor (1972) and Chandra (1974) have shown data from OGO's 4 and 6 ion mass spectrometers which confirm the He^+ and O^+ nighttime distributions shown here. Chandra relates the behavior of these distributions to the geomagnetic anomaly, the electrodynamic lifting of ionization in the equatorial region and its subsequent diffusion along the field lines. As the spacecraft cuts across field lines, the observed ion concentration distribution reflects the vertical profile of each constituent at the equator.

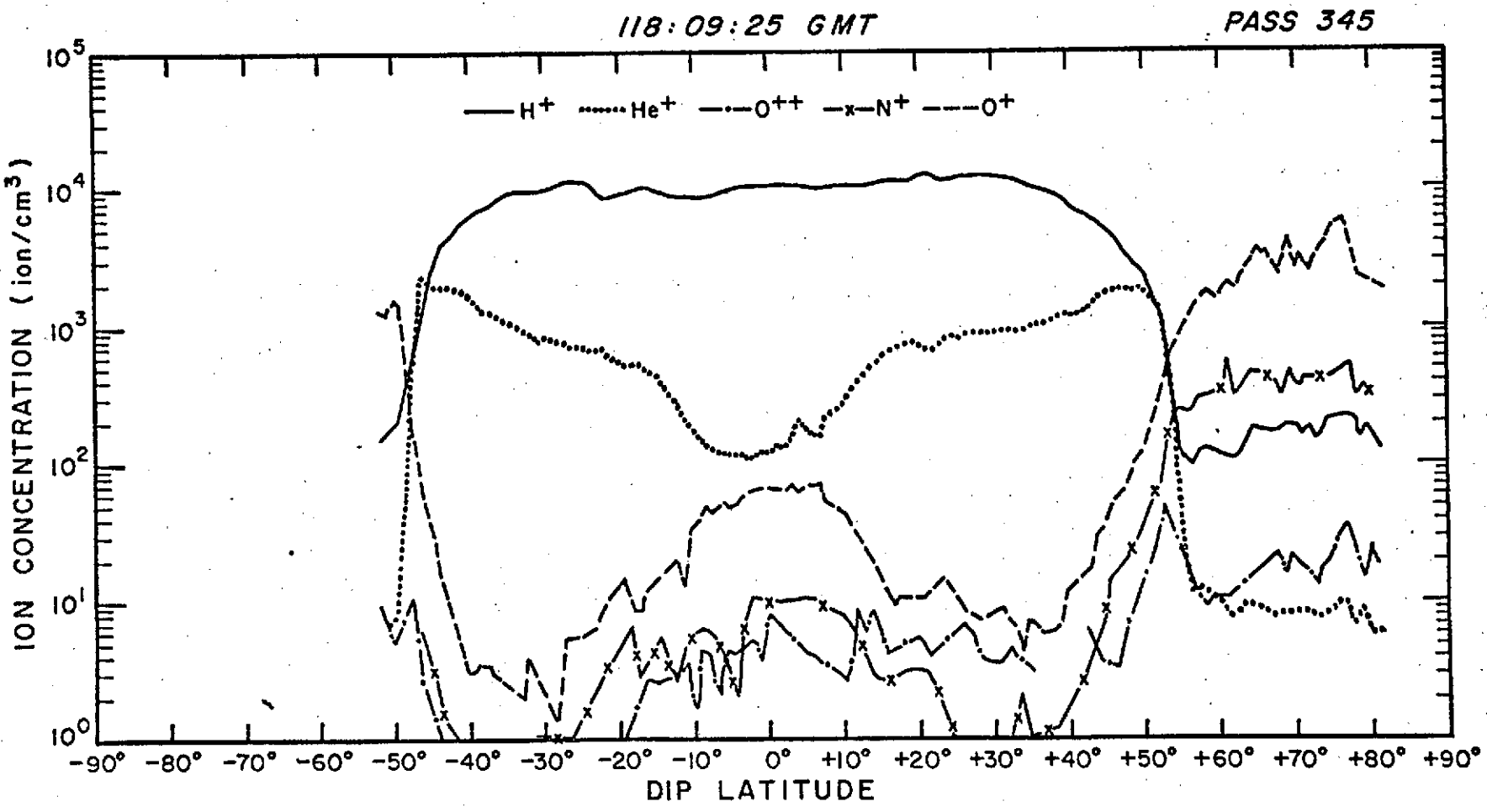

Figure 3

Nighttime pole-to-pole plot of ion composition at 1400 km and 0500 LT. Summer is to the right; winter to the oeft.

O^{++} generally follows O^+ at a concentration level 100 to 200 times lower in summer daytime, but approaches the O^+ value in the winter trough. In the nighttime midlatitude regions where O^+ is less than 10 ions cm^{-3}, O^{++} lies within a factor of 3 of O^+, especially in the summer. At higher latitudes where O^+ becomes dominant, the nighttime ratio returns to the order of 100.

N^+ ions seem to track O^+ rather consistently at roughly one order of magnitude lower concentration except at mid to low latitude daytime (Figure 1) where the O^+/N^+ ratio is more like 20, and at night (Figure 3), where, on each side of the equatorial O^+ maximum, the ratio is as low as 3. However, at these exceptional times, the N^+ concentration is of the order of 5 ions cm^{-3} making the uncertainty in the measurements greater, but still probably less than 50%.

1.2 POLAR WIND

In addition to providing data on the composition of the ionosphere the mass spectrometer data were used to define the existence of a flow of light ions with respect to heavy ions and thus to determine the mean velocity of the light ions. Observations were made of the flow velocities and fluxes of light ions (hydrogen and helium), called the Polar Wind, through an assumed static distribution of oxygen ions. The Explorer XXXI mass spectrometer provided the first experimental evidence for the existence of the polar wind; the ISIS-II instrument enabled continuing observations of the distribution and magnitude of the phenomenon.

Evidence for the polar wind is seen in roll modulation plots like that of Figure 4. Only O^+, He^+ and H^+ are shown for clarity. All the ion species normally appear on this type of plot. The data clearly show the roll modulation effect of a spinning satellite. If all the ion species have merely thermal velocities, the roll modulation maxima will be coincident in time and coincide with the ram direction (zero angle of attack). See

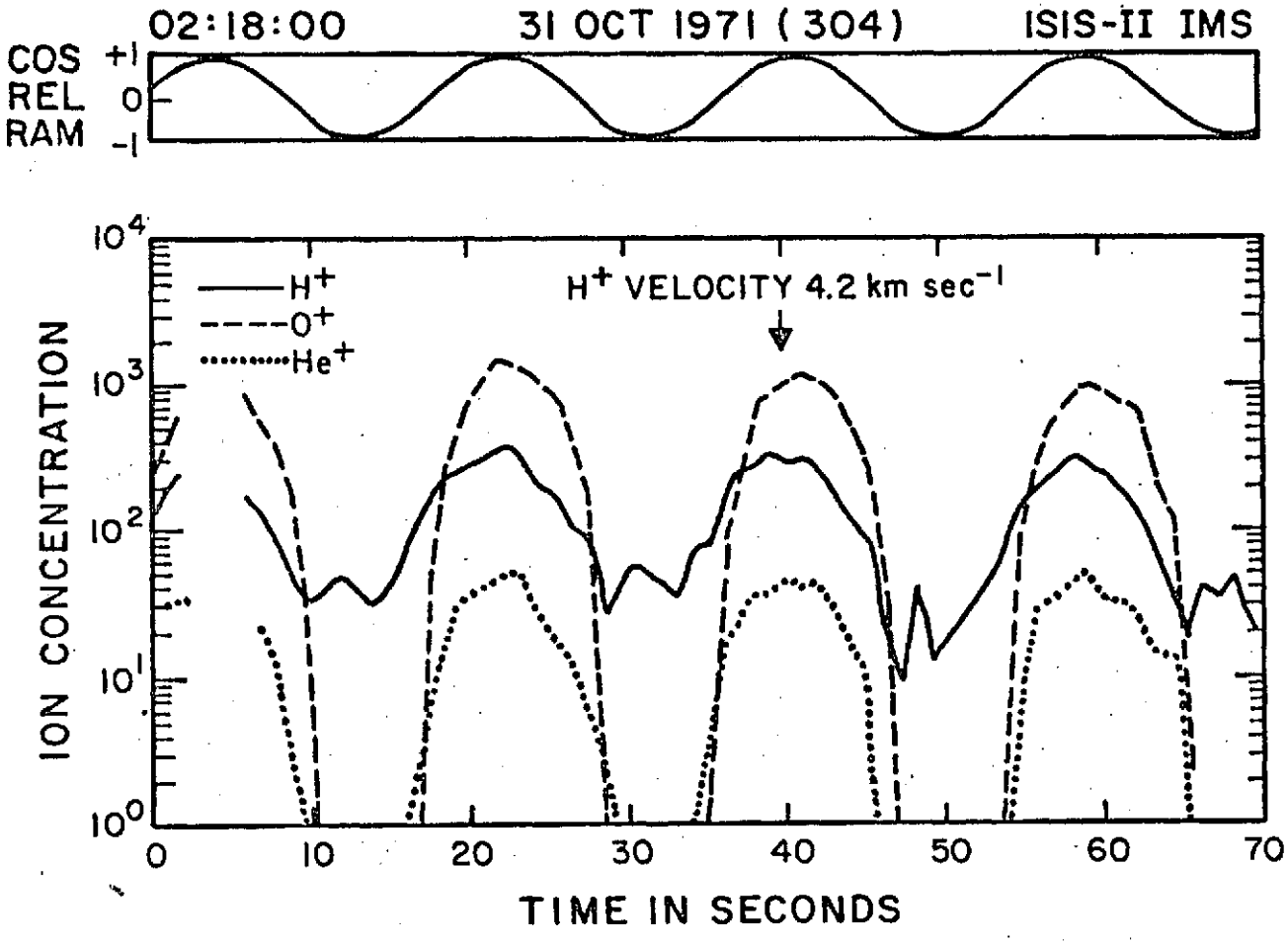

Figure 4.

Roll modulation curve showing ion concentrations as a function of time with ephemeris data along abscissa. When cosine of relative ram angle is 1.0, angle of attack is zero. Phase shift between O^+ and H^+ roll modulation maxima is measure of the polar wind velocity.

cosine curve in Figure 4. However, if one ion species velocity contains a bulk motion term, its maximum will be shifted away from ram in the direction of the resultant between the satellite velocity and bulk velocity vectors. By observing the magnitude of this phase shift, and knowing the satellite velocity, the bulk velocity can be calculated. Polar wind velocities are easily measured by this process. In the example of Figure 4, the H^+ velocity is 4.2 km sec^{-1} and the H^+ flux is 1.3×10^8 ions $cm^{-2}sec^{-1}$.

He^+ also frequently exhibits a phase shift with respect to O^+ and the ram direction with a magnitude usually about one half that of H^+. In the present example, the He^+ velocity and flux are 2 km sec^{-1} and 9×10^6 ions $cm^{-2}sec^{-1}$ respectively.

The polar wind generally occurs poleward of the plasmapause and is thought to be the flow of light ions along open magnetic field lines out into the tail of the magnetosphere. It appears to flow essentially at all times and is found to be very strong in the cleft region but is certainly not confined to it. The polar cap region tends to be devoid of ionization and therefore, any polar wind flows in this region cannot be measured since the concentrations of the light and heavy ion species are insufficient to determine the roll modulation phase shifts. In addition to this general transplasmapause polar wind there appear to be strong H^+ fluxes at the equatorward edge of the plasmapause. Generally, the velocities are low in this region but the concentrations being fairly high give rise to substantial fluxes. It is thought that in this region the ion fluxes are refilling the magnetic field tubes which have been depleted of ionization after they have opened into the magnetospheric tail.

The summer daytime plasmapause and transplasmapause regions are characterized by little structure and no trough in the O^+ concentration. This concentration is of the order of 10^4 ions cm^{-3}. Generally, the H^+

velocities and fluxes poleward of the plasmapause are quite small. The H^+ concentrations in this region are of the order of 10^2 to 10^3 ions cm^{-3}. At times there is a small enhancement in the O^+ concentration (like a factor of 2 or 3) near 75 to 80^o invariant latitude which seems to be somewhat correlated with precipitating energetic particles in this region. There is also a small enhancement in the electron temperature.

In the winter day there is observed a very deep trough in the H^+ and O^+ concentrations between the plasmapause and the cleft. Then the cleft shows a large enhancement in O^+, these concentrations reaching of the order of 10^4. In the cleft region there are also large hydrogen velocities giving rise to substantial upward fluxes of hydrogen ions.

In the nighttime, a large H^+ concentration trough is seen just poleward of the plasmapause in both the summer and winter hemispheres. In the summer, O^+ concentrations are very low (less than 10 ions cm^{-3}) equatorward of the plasmapause, whereas poleward they rapidly increase to between 10^3 and 10^4 ions cm^{-3}. These large O^+ enhancements are correlated with large particle precipitation fluxes. The high concentration region of O^+ extends generally into the polar region where there is little evidence of a polar cavity. Also, the H^+ fluxes and velocities are low giving rise to very small polar winds. In the winter night however, there are very large H^+ velocities poleward of the trough where the O^+ enhancement occurs. In this case though, there is a deep polar cavity essentially devoid of ionization. Again, as in summer the O^+ concentration equatorward of the plasmapause is very low.

1.3 WAKE STUDIES

The H^+ wake enhancement seen in the polar wind plots of Figure 4 is a commonly observed phenomenon but its origin has not been studied in detail. A number of satellite wake studies have been conducted, but these

are mainly theoretical and very little comparison between theory and experiment has been done (Samir and Jew, 1972). From the data exhibited here, it appears that the light ions are capable of reaching the instrument when it is pointing in the wake, as has been shown by Samir et al. (1973), and in certain preferred directions (Not exactly in the wake) there appears to be a channel through which ions are more readily transported to the instrument.

1.4 MAGNETIC STORM EFFECTS

The general behavior of the ionosphere is as shown in Figure 1 with O^+ as the dominant ion species throughout most of the daytime and N^+ roughly one order of magnitude lower. The tracking of N^+ with O^+ is typical of all quiet time ionospheres. However, during the greatly disturbed time of the August 1972 magnetic storm, at about 1700 local time, August 4, N^+ becomes the dominant ion, exceeding O^+, from 55° invariant latitude toward the pole as is shown in Figure 5. During this time the 3 hour K_p index was 9. At the same time, the three molecular ion species, N_2^+, NO^+ and O_2^+ are observed for the first time at 1400 km. Under normal conditions they are below the detection limit, 1 ion cm^{-3}, of the instrument. Concentrations in the 10^3 cm^{-3} range are, therefore, highly unusual, as is the N_2^+ dominance over the other molecular species. In the normal E and F regions, N_2^+ is a very minor species compared with NO^+ and O_2^+ ions, while formed by photoionization in the 150 to 200 km range, rapidly charge exchange with O and O_2 forming NO^+ and O_2^+.

Data from the ESRO IV mass spectrometer (Prölss and von Zahn, 1974) have shown a marked decrease in the neutral O/N_2 ratio and a corresponding enhancement of neutral N_2 at relatively high altitudes during the large magnetic storm ($K_p=7^+$) of February 21, 1973. (No neutral composition data are available for the August 1972 storm). The excess high altitude N_2 is ionized, but, because neutral gas concentrations (O and O_2) above 300 km

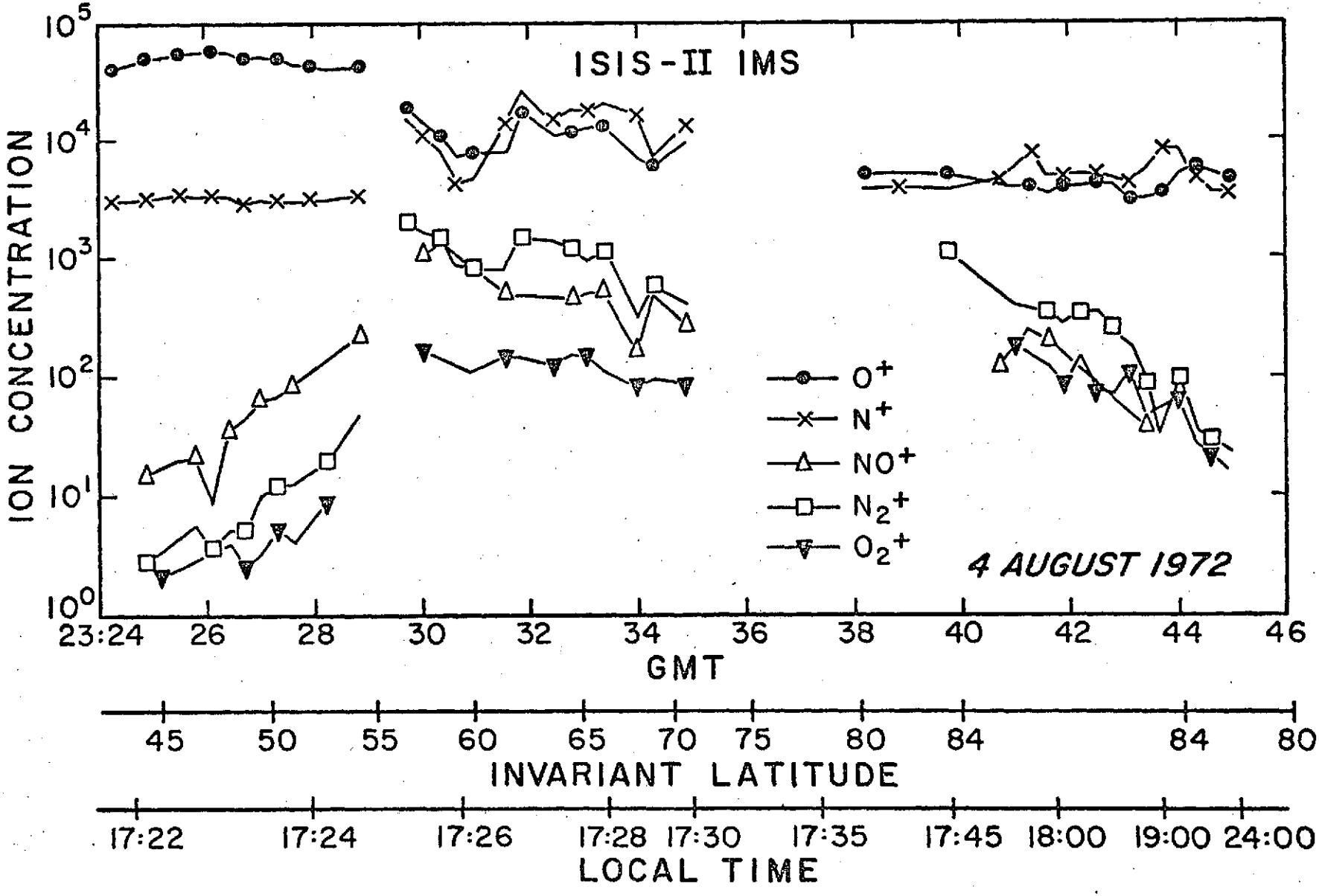

Figure 5.

Ion composition during August 1972 magnetic storm. Note N^+ dominance and high concentrations of molecula ion species. Because the plasmapause is highly depressed in latitude (L=3.0), the molecular ion region lies in the trans-plasmapause region.

are much less than in the 150-200 km range, the charge exchange reactions cannot proceed as rapidly, leaving much of the ionization in the form, N_2^+. The high molecular ion concentrations are further supported by the high ion temperature, approximately 4000 K, measured during this phase of the storm. (E. Maier, private communication). Taylor (1973) observed from the OGO-6 satellite a large enhancement of NO^+ during the storm of March 8, 1970 at an altitude of 400 to 600 km (it is not clear from the reference that N_2^+ and O_2^+ are also enhanced at this time). In that case O^+ remained the dominant species instead of N^+ which may be due to the fact that Taylor's measurements were at a lower altitude, or that the magnitude of the 1970 storm may have been less than the 1972 storm. Simultaneous measurements from the OGO-6 neutral mass spectrometer showed an N_2 enhancement confirming the ESRO IV results.

Essentially all of the region at 1400 km where molecular ions are important lies above the plasmapause, located by a steep negative gradient in H^+, which in this case occurred at 55^o invariant latitude (L=3). The ISIS IMS data in Brace, et al, (1974), shows that during various phases of the storm's development the plasmapause was depressed as far south as L=1.9. The H^+ concentration remains rather low ($<10^2 cm^{-3}$) throughout the polar region but begins an upward trend towards the night side of the polar cap where the molecular species are rapidly disappearing.

1.5 POLAR AURORA AND AIRGLOW

The IMS in conjunction with other experiments on board the ISIS-II spacecraft has been used in a study of the polar aurora and airglow. Spin maps for the 6300Å, 5577Å and 3914Å airglow emission were made for a south pole pass on April 23, 1971. These data were correlated with the ion densities and temperature and electron temperature from the direct measurement experiments on the spacecraft. Likewise, ion composition

results were also correlated with the remainder of the data. A large peak in the 5577Å intensity shows a strong correlation with an enhancement in O^+ concentrations and a corresponding decrease in H^+ concentration at about 70^o invariant latitude. This region which lies beyond the plasmapause and the H^+ trough typically exhibits a pronounced peak in O^+. The electron and ion temperatures tend to show a sharp peak up to nearly 4000^oK, very near the bottom of the H^+ trough. The correlation of these results is discussed in a paper by Shepherd, et al (1973).

2.0 INSTRUMENTATION

The Ion Mass Spectrometer was designed and built at UTD and integrated into the ISIS spacecraft at the spacecraft contractor's plant (RCA) in Montreal. The instrument is a miniature magnetic deflection mass spectrometer designed to identify and measure the concentration of positive ions in the earth's upper atmosphere in the mass range 1 to 64 amu.

It consists of an entrance aperture, magnetic mass analyzer and ion detection system as shown in Figure 6. The entrance aperture, a 7.6 cm diameter screen mounted flush with the spacecraft surface, is oriented to look radially outward from the spacecraft. Ambient ions are attracted to the screen by a -6 volt potential on the screen and by the usually negative satellite potential.

There are two basic orientation modes of the spacecraft, cartwheel and orbit-aligned. In the former, the spin axes is normal to the orbit plane allowing the spacecraft to roll (or skid) along the orbit such that the entrance aperture points alternately in the ram and wake directions. In the latter the spin axis lies in the orbital plane. The satellite velocity, which is large compared to ion thermal velocities (except for H^+) generates an ion flux toward the satellite in the reference frame in which

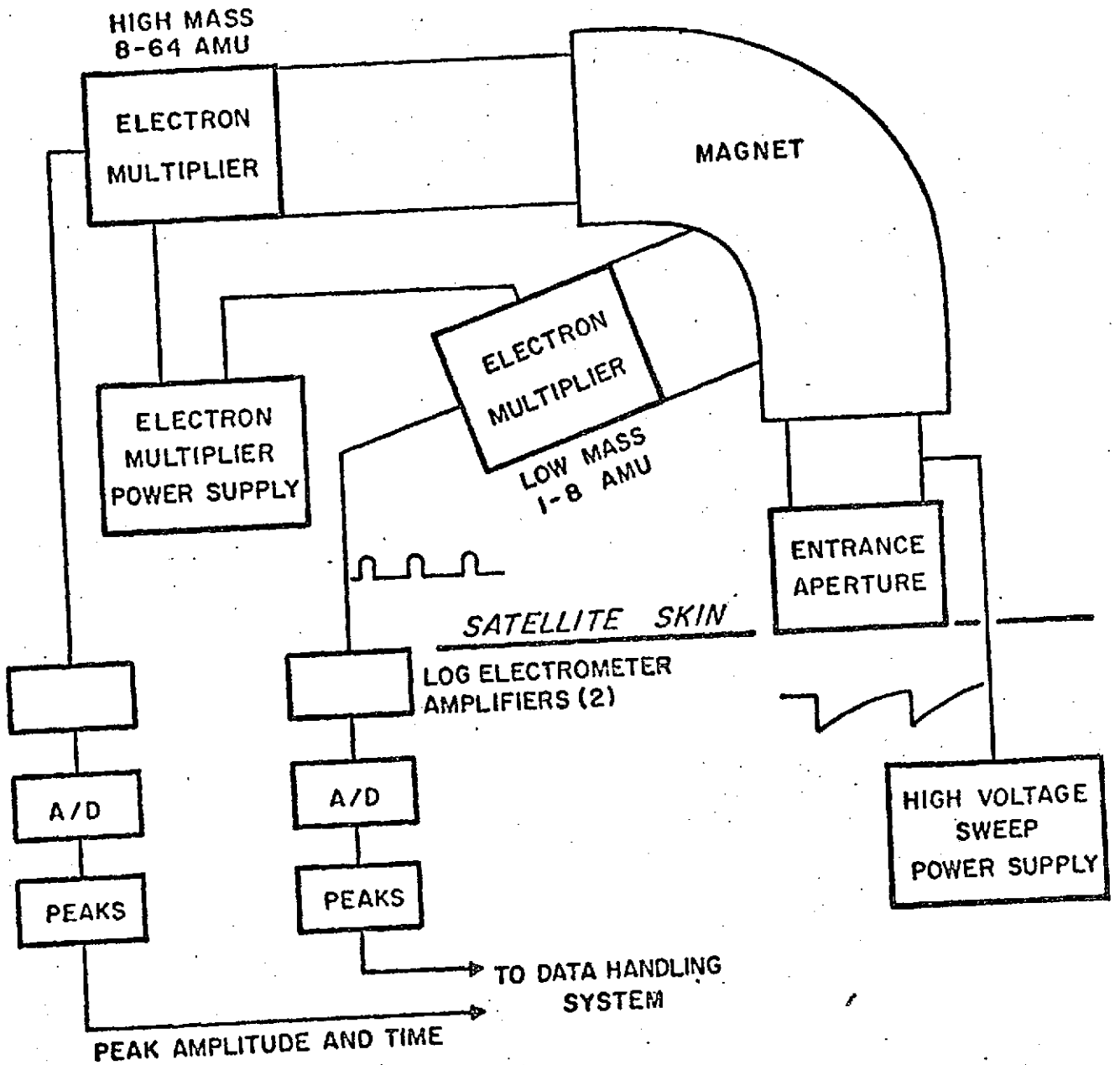

Figure 6

ISIS-II ion mass spectrometer showing principal parts of instrument and major electronic assemblies. Use of two detector channels permit simultaneous scanning of two parts of mass spectrum enabling the entire mass range from 1 to 64 amu to be swept in one second. Instrument is packaged in a rectangular box 15 cm x 12.5 cm x 33 cm weighing 6.1 kg. and mounted behind an equatorial panel of the spacecraft to look radially outward.

the satellite is at rest. Since the portion of this flux which passes into the mass spectrometer is a strong function of angle of attack of the entrance aperture, the spinning motion of the spacecraft produces data which is roll modulated with the modulation amplitude (ram to wake ion current ratio) being strongly mass dependent. Valid ion concentration data are obtained only when the angle of attack is near zero, the ram condition. The orbit-aligned case produces a favorable angle of attack only at 2 points along the orbit, the positions depending on the declination of the spin axis. For this reason, data presented herein have been taken only when the satellite is in cartwheel mode, in which the satellite was operated about 50% of the time.

Ions which pass through the entrance screen are accelerated through a narrow slit (the object slit), collimated into a beam and passed through the magnetic analyzer. Two allowable ion trajectories, 1.8 and 5.1 cm radii, through the magnetic field lead to two collector slits positioned such that ions of mass ratio 1 to 8 can simultaneously reach the slits. The mass spectrum is scanned by varying the ion accelerating voltage, which has a repetitive exponentially decaying wave form with a 1 second period, over the range from 2000 to 250 volts. This causes the mass ranges 1 to 8 and 8 to 64 amu to be simultaneously swept across the collector slits once each second.

Ions traversing each collector slit are detected by a magnetic strip electron multiplier (Bendix M310S), used as a current amplifier, and a logarithmic electrometer amplifier, one for each mass range. The dynamic range of each log amplifier is 2×10^{-12} to 1×10^{-6} amp producing an output voltage range from 0.2 to 5.0 volts. Sensitivity of the instrument in flight is a few tenths of an ion cm^{-3}, this very high sensitivity being due in part to the rapid motion of the satellite through the ionospheric medium.

The signals from each log amplifier are digitized to 8-bit words and fed into "peaks" circuits which detect the mass spectral peak amplitudes by a logic process involving peak location and amplitude averaging. The "peaks" circuit is a unique feature of this instrument. It searches the output data from the log amplifiers for bonafide peaks (noise spikes are rejected) and determines the amplitude of each. Subsequently these amplitudes are stored in buffer registers until sampled by the telemetry system. Since only the peak amplitudes are transmitted, a relatively small bandwidth suffices to read out the data. By using this technique, the short sweep time of one second can be effectively utilized to produce 15 to 20 data points for each spectral peak for each satellite roll period (depending on spin rate). This data rate is sufficient to adequately define the roll modulation curve for each ion species. The position of each ion peak in the telemetry format determines its mass number.

A backup-diagnostic mode, called the analog mode, is available in which the spectral scan time is increased to 8 seconds, the "peaks" circuits are disabled, and the entire mass spectrum is telemetered. This mode is used once each week for two minutes to monitor instrument operation via a quick-look data handling process. Figure 7 is a block diagram of the electronics.

2.1 Instrument Calibration

An ion mass spectrometer measures relative abundances of the ions sampled from the ionosphere but can be calibrated to give absolute ion concentrations. Several factors cause the spectrometer to discriminate against ions of heavy mass. First, the instrument scans the mass spectrum by varying the ion accelerating voltage in an exponential manner from 2000V to 250V. Lower mass ions are measured near the high voltage end of the

BLOCK DIAGRAM OF INSTRUMENT ELECTRONICS

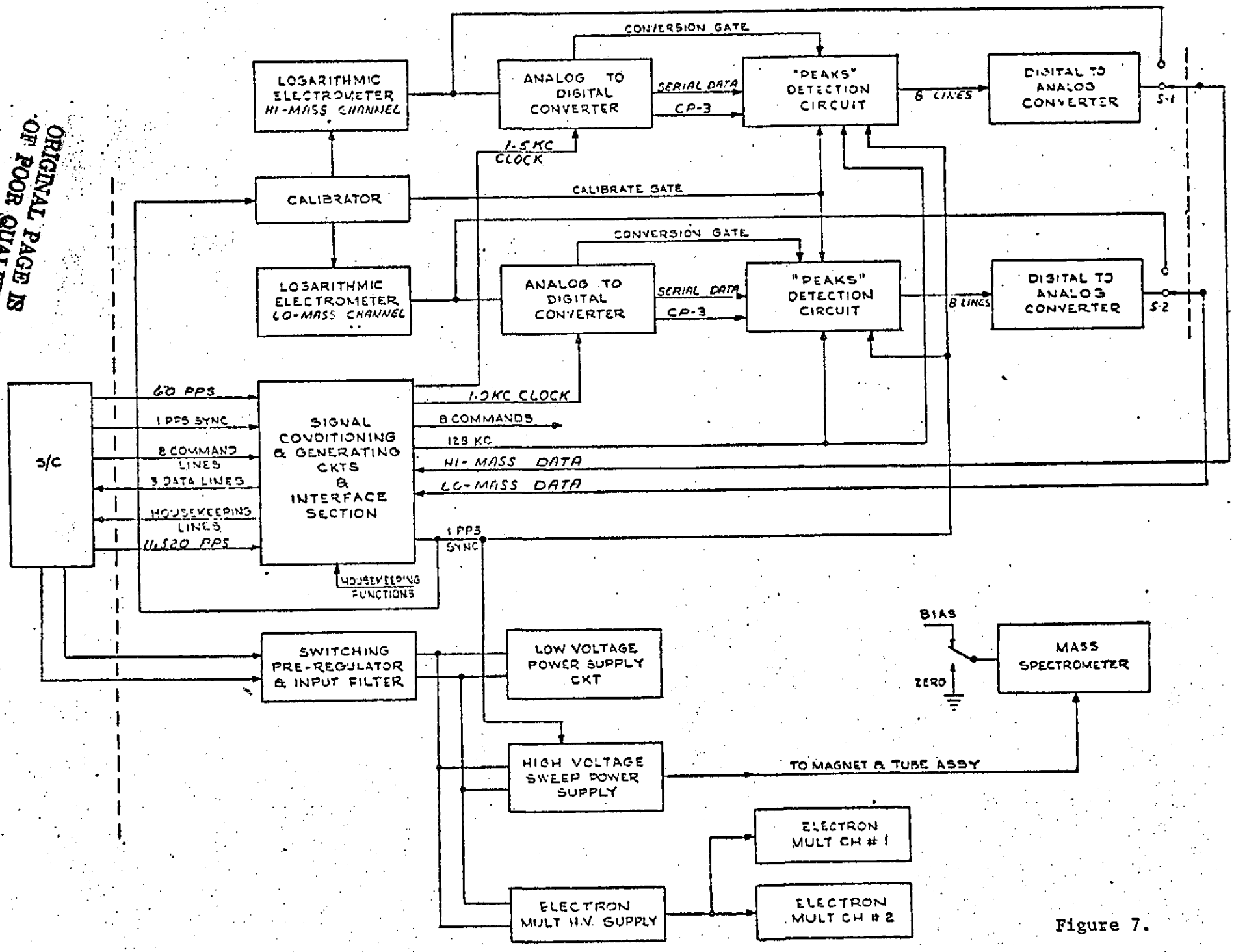

Figure 7.

sweep where the instrument has a higher transmission factor than at the low voltage/high mass end. This phenomenon is known as the voltage effect. Second, light mass ions, being more mobile than heavy mass ions, are collected from a larger volume. Hence, a larger light mass ion current is measured for equal concentrations of light and heavy mass ions.

The only practical method of calibration of an ion mass spectrometer is an in-flight procedure (Hoffman, 1969; Hoffman et al, 1973) in which the sampling efficiency of the various ion species from the plasma was done by comparing the total ion current (the sum of all the peaks) with electron density data from the ionograms produced from the sounder experiment on board ISIS-II (J. Whitteker, private communication). Comparisons were first made in regions where the ionosphere consisted of greater than 95% H^+ ions (the remainder being mainly He^+ and D^+). Thus, a direct calibration of the absolute sensitivity of the mass spectrometer to H^+ was obtained. Next, a similar calibration was made for O^+ using ionospheric regions that were greater than 90% O^+. In this case the calibration for H^+ was incorporated into the calculation. He^+ calibration had been inferred from the above, but recently a region of He^+ dominance was identified and a direct He^+ calibration obtained. From the 3 point calibration, the sensitivity factors for the minor ions were obtained.

A typical example of the result of this in-flight calibration procedure is shown in Figure 8. In pass 339, the ion composition changes from predominantly O^+ to H^+ at -5^o and back to O^+ at -45^o latitude. In pass 345, the composition changes from predominantly H^+ below to O^+ above 55^o latitude. Figure 3 shows the detailed composition of this pass. Agreement between the total ion concentration, N_i, as determined by the sum of the individual ion species concentrations, and the electron density is generally

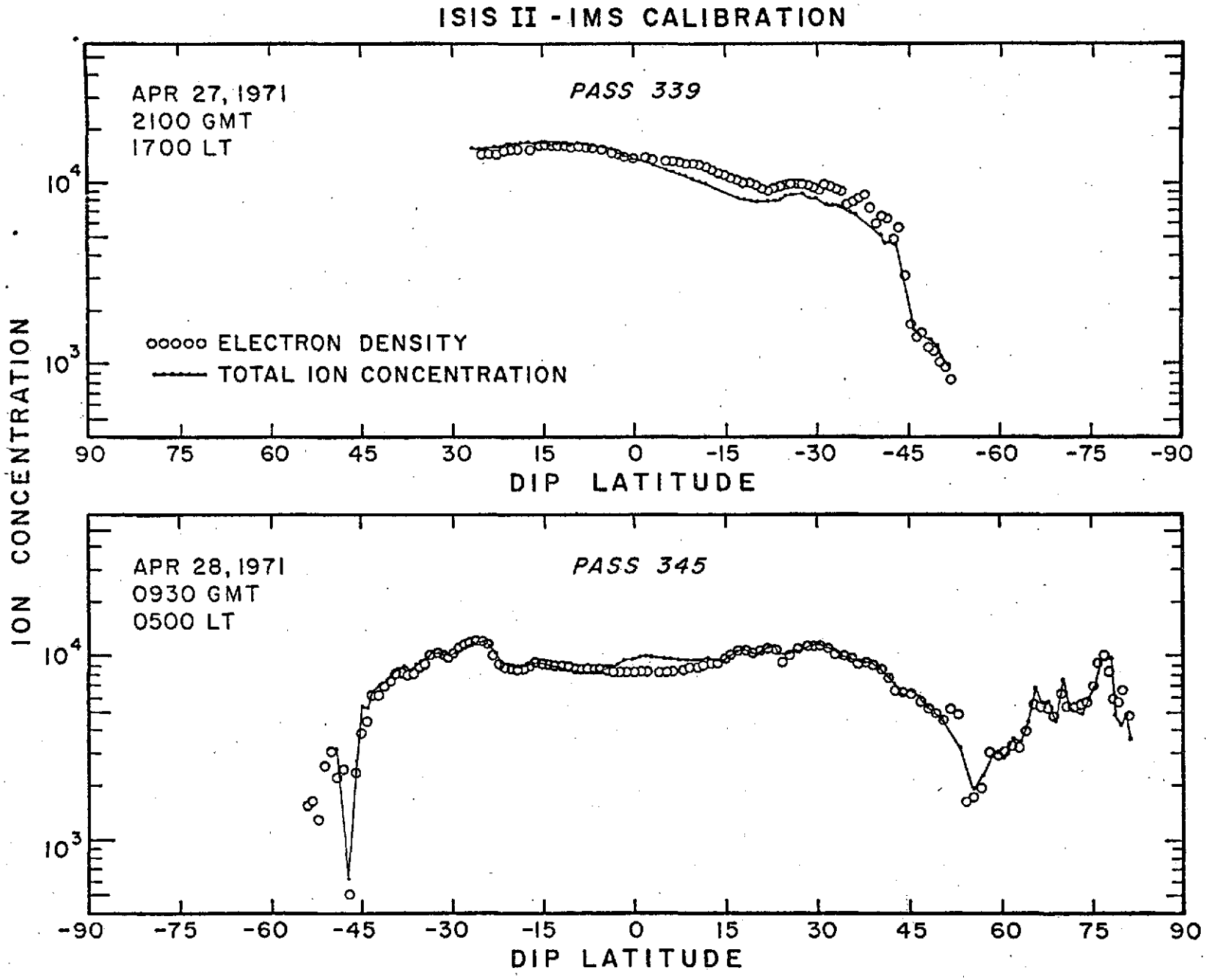

Figure 8.
In-flight calibration result showing comparison of total ion composition and electron density from on-board topside sounder. Agreement is generally better than 10%. In pass 339, the ion composition is predominantly H^+ between -5° and -45° latitude and O^+ both farther northward and southward. Composition changes from dominantly H^+ below to O^+ above 55° Lat. in pass 345.

better than 20% regardless of which ion is the dominant species except perhaps in highly structured regions.

The mass spectrometer measures the ionospheric parameters in the immediate vicinity of the spacecraft. That is, it can only detect those ions which arrive at the instrument entrance aperture, whereas, the sounder electron density measurement is an integral result of the electron density near the spacecraft. In highly structured regions, these two may not always track. In addition, the calibration coefficients (sensitivity factors), which are determined by this comparison process, are thought to be somewhat dependent on total ion density and composition, ion temperature and spacecraft potential (Parker and Whipple, 1970; Whipple et al. 1974). Nevertheless, these effects seem to be sufficiently small to enable the mass spectrometer to produce ion concentration measurements to better than 20% accuracy as compared with simultaneous electron concentration data, such as obtained from the topside sounder.

3.0 FUTURE WORK

A wealth of data has been obtained from the ISIS-IMS, much of which has yet to be studied. A number of tasks have been proposed and funded through a grant from NASA. These are discussed below.

3.1 Polar Wind

The polar wind plasma flows have definitely been found in the cleft region but are certainly not confined to it. The plasma pause is frequently observed to lie between 55° and 60° invariant latitude. However, a strong upward flux of hydrogen ions is frequently observed at the equatorward edge of the plasma pause. This plasma pause boundary moves towards the equator during a magnetic storm. New field lines then open to the tail causing

large fluxes of hydrogen ions to flow to the tail region emptying these field tubes. When these field lines reconnect, plasma begins to flow up along the field line refilling them. Since the mean time between substorms is longer than the filling cycle of flux tubes, there is a continuous filling of these tubes and a rather continuous flow of polar wind particles which can often be along closed field lines. In the winter polar wind velocities tend to be larger than in summer time but confined to a narrower region, while in the summer the area is quite broad with fairly low velocities. Also in the winter there is a very marked polar cavity essentially devoid of ionization. Whereas the summer polar cap region contains a broad region of O^+ dominance of the order of 10^4 ions cm^{-3}.

One of the tasks which is proposed to be conducted at UTD during the next year is strongly oriented toward continuing the study of the polar wind, for which a wealth of data exists and a major paper is under preparation.

3.2 Disturbed Ionosphere

A study involving ESRO IV neutral mass spectrometer results (Prölss and von Zahn, 1974) and ISIS-II ion mass spectrometer data during the magnetic storm of February 1973, will be initiated with the view to determining the correlation between the enhancement of the neutral species, particularly N_2, and the changes in ion composition observed during a large magnetic storm.

3.3 Global Helium Study

A cooperative program with J. Lemaire of the Institut D'Aeronomie Spatiale De Belgique of Brussels has been initiated to study the global distribution and escape rates of helium from the exosphere. UTD will

select and analyze data with respect to upward flows of helium ions while Lemaire will interpret the results in terms of a model to determine the global escape rates of helium.

3.4 Cooperative Projects with Other ISIS Team Members

Data has been supplied to Leroy Smith of the Battelle Northwest Institute who is working with C. Anger on studies of auroral region airglow. We have and will continue to supply the data taken from satellite passes in the region near the Battelle Institute in Washington and the Alaska ground stations.

Data will be supplied to G. Shepherd to compare cleft responses of all instruments on the ISIS-II satellite to look for correlative effects between all of the ionospheric parameters measured by the ISIS-II instruments as related to the cleft region.

A study is being initiated in which several pole-to-pole passes for which good values of ion composition, T_e, T_i and good electron density profiles are available will be compared with data from radar back scatter stations such as Arecibo and Millstone. From the satellite data it should be possible to calculate vertical profiles of composition and temperature and compare these to similar data obtained by the back scatter techniques.

Another correlative venture will be to obtain as much data as possible from the ISIS-I and ISIS-II spacecrafts to give as comprehensive a picture as possible of the winter polar cap ionosphere and compare these data to ground stations available in these regions.

3.5 Atmospheric Explorer Comparisons

A large effort is mounting toward cooperative comparisons of data with results from the AE-C spacecraft, particularly the ion mass spectrometer

(MIMS) and the retarding potential analyzer (RPA), both UTD experiments. Coincident passes are being scheduled as frequently as possible. Since ISIS-II is in a circular (1400 km) orbit and AE-C is in a highly elliptical orbit, coincident passes will likely give results at 2 widely separated altitudes, with the top side sounder providing altitude profiles of electron density between the respective satellite altitudes. This phenomenon will be particularly true after the AE-C orbit is circularized at 250 to 300 km altitude, which has occurred in early 1975.

These AE cooperative ventures will be directed, first of all toward a cross calibration of the two ion mass spectrometers, then a continuation of the study of the polar wind, and equatorial ionospheric phenomena (e.g. spread-F). It is expected that a number of useful studies will result from the interaction of the ISIS and AE teams, particularly since two of the team members are common (Hoffman and L. Brace) and one ISIS experimenter (G. Shepherd) is an AE Co-investigator.

References

Brace, L. H., E. J. Maier, J. H. Hoffman, J. Whitteker, and G. G. Shepherd, Deformation of night side plasmasphere and ionosphere during August 1972 geomagnetic storm, J. Geophys. Res., submitted, 1974.

Breig, E. L. and J. H. Hoffman, Variations in ion composition at mid- and low-latitudes from ISIS-II satellite, J. Geophys. Res., 1975, to be published.

Chandra, S., The equatorial helium ion trough and the geomagnetic anomaly, J. Atmo. Terr. Phys., in press, 1974.

Hoffman, J. H., Ion mass spectrometer on Explorer XXXI satellite, Proc. IEEE, 57 (6), 1063, 1969.

Hoffman, J. H., W. B. Hanson, C. R. Lippincott, and E. E. Ferguson, The magnetic ion-mass spectrometer on atmospheric explorer, Radio Science, 4, 315, 1973.

Parker, L. W., and E. C. Whipple, Jr., Theory of spacecraft sheath structure, potential, and velocity effects on ion measurements by traps and mass spectrometers, J. Geophys. Res., 75, 4720, 1970.

Prolss, G. W. and U. von Zahn, ESRO IV gas analyzer results, 2, direct measurements of changes in the neutral composition during an ionospheric storm, J. Geophys. Res., to be published, 1974.

Samir, U., E. J. Maier and B. E. Troy, Jr., The angular distribution of ion flux around an ionsopheric satellite, J. Atmo. Terr. Phys., 35, 513, 1973.

Samir, U., and H. Jew, Comparison of theory with experiment for electron density distribution in the near wake of an ionospheric satellite, J. Geophys. Res., 77, 6819, 1972.

Shepherd, G. G., C. D. Anger, L. H. Brace, J. R. Burrows, W. J. Heikkila, J. H. Hoffman, E. J. Maier, and J. H. Whitteker, An observation of polar aurora and airglow from the ISIS-II spacecraft, Planet. Space Sci., 21, 819, 1973.

Taylor, H. A., Jr., Storm-time relationships observed between H^+ and NO^+, some implications for chemistry and dynamics, EØS, 54, No. 4, 386, 1973.

Taylor, H. A., Jr., Observed solar geomagnetic control of the ionosphere: implications for reference ionospheres, Space Res., XII, 1275, 1972.

Whipple, E. C., J. M. Warnock, and R. H. Winkler, Effect of Satellite potential on direct ion density measurements through the plasmapause, J. Geophys. Res., 79, 179, 1974.

4.0 BIBLIOGRAPHY

The following papers have been prepared, to date, from scientific data resulting from the ISIS-II Ion Mass Spectrometer Experiment.

a. Breig, E. L., J. H. Hoffman and W. H. Dodson, Mid- and low-latitude ionospheric concentrations and variabilities at 1400 km, Trans. Am. Geophy. Union, 54, No. 43, 385, 1973.

b. Breig, E. L. and J. H. Hoffman, Variations in ion composition at mid- and low-latitudes from ISIS-II satellite, submitted to J. Geophys. Res., 1975, to be published.

c. Brace, L. H., E. J. Maier, J. H. Hoffman, J. Whitteker, and G. G. Shepherd, Deformation of the nightside plasmasphere and ionosphere during the August 1972 geomagnetic storm, submitted to J. Geophys. Res., 1974.

d. Dodson, W. H. and J. H. Hoffman, Ion composition measurements from ISIS-II satellite (abstract), EØS Trans. AGU, 54, 384, 1973.

e. Hoffman, J. H., Studies of the composition of the ionosphere with a magnetic deflection mass spectrometer, Int. J. Mass Spectrum, Ion Phys., 4, 314, 1970.

f. Hoffman, J. H., The polar wind, Magnetospheric Cleft Symposium, University of Texas at Dallas, November 1973; EØS, 55, 69, 1974.

g. Hoffman, J. H., W. H. Dodson, C. R. Lippincott, and H. D. Hammack, Initial ion composition results from the ISIS-II satellite, J. Geophys. Res., 79, 4246-4251, 1974.

h. Maier, E. J. and J. H. Hoffman, Observation of a two temperature ion energy distribution in regions of polar wind flow, J. Geophys. Res., 79, 2444, 1974.

i. Shepherd, G. G., C. D. Anger, L. H. Brace, J. R. Burrows, W. J. Heikkila, J. H. Hoffman, E. J. Maier, and J. H. Whitteker, An observation of polar aurora and airglow from the ISIS-II spacecraft, Planet. Space Sci., 21, 819, 1973.

Papers identified in b, g and h above are included as appendices A through C to this final report.

APPENDIX A

VARIATIONS IN ION COMPOSITION AT MID AND LOW LATITUDES FROM ISIS-II SATELLITE

E. L. Breig and J. H. Hoffman

The University of Texas at Dallas

Richardson, Texas 75080

September 12, 1974

December, 1974

Submitted for Publication

in

Journal of Geophysical Research

ABSTRACT

The ion mass spectrometer onboard the ISIS-II satellite has provided detailed information on absolute concentrations of the principal ion species near the fixed altitude of 1400 km. This analysis describes the latitudinal and longitudinal variations of such concentrations for dip latitudes below 50°, in the afternoon (14-17.5 hr) and predawn (02-05.5 hr) local times, during undisturbed seasonal periods characteristic of late April/early May. The predawn level of ionization at 1400 km is comparable to that observed in the afternoon. Although H^+ is the dominant nighttime ion, the principal predawn longitudinal variations relate to the seasonal asymmetry of O^+, and to the shape and extent of the low-latitude He^+ depressions. Two distinct classes of daytime ionospheric behavior are observed. Certain longitude regions are distinguished by broad summer plateaus of O^+, separated by sharp equatorial gradients from concentration depressions at winter latitudes. O^+ and H^+ are the major species in the summer and winter hemispheres, respectively, while He^+ exhibits the characteristic equatorial trough. Alternatively, a region of longitude has been observed where the seasonal variation of O^+ is less pronounced, and where He^+ possesses a symmetrical peak at the dip equator. Both direct photoionization processes and neutral winds are considered capable of producing these daytime effects. The data confirm the strong solar-geomagnetic seasonal control over the topside ion distribution. More-comprehensive comparisons of ion profiles between different longitudes and seasons are possible when the magnetic dip equator is adopted as reference for the solar direction and hence for the effective ionospheric season.

INTRODUCTION

Although the identities of the major ionic species in the undisturbed topside ionosphere have now been firmly established, observational data are still not sufficiently extensive to allow a detailed generalization of the diurnal, seasonal, latitudinal and longitudinal changes in the ion composition at these altitudes. Data directly related to such ionospheric variations have been recently reported from instruments onboard the OGO-4 (Chandra et al., 1970; Taylor, 1971) and OGO-6 (Taylor, 1972) satellites. References to earlier experimental observations and a discussion of the status of current understanding of the normal ionosphere above the F_2 peak, especially at low and mid latitudes, are also included in the analyses of these authors.

Chandra et al. (1970), in presenting results from the retarding potential analyzer on OGO-4, placed emphasis on the variation with latitude of the principal ion concentrations and the charged particle temperatures, at low and mid latitudes near the fall equinox. An analysis of data from the ion mass spectrometer onboard the same spacecraft (Taylor et al., 1970) has suggested the existence of a strong longitudinal variation in the concentrations of the major ions near the 900 km orbital apogee. Taylor (1971) presents a more detailed description of this behavior for local noon in late May and in the late afternoon near solstice. The latter studies include the high latitude trough region, and demonstrate the solar-geomagnetic seasonal control of the ion composition at these altitudes. This type of analysis has been extended by Taylor (1972) to the ion mass spectrometer data near the 1100 km orbital apogee of OGO-6, with discussion of selected orbits of late afternoon, midnight and predawn data. However, the above analyses were limited in their local time and seasonal coverage, and the nature of

the OGO-4 and OGO-6 orbits prevented a complete decoupling of the altitude dependence.

This paper describes absolute ion concentration measurements with an ion mass spectrometer on the ISIS-II satellite, and discusses features of the ion composition near a fixed altitude of 1400 km as they relate to longitudinal and latitudinal variations at low and mid latitudes. These data, in general, complement the OGO-4 and OGO-6 results, being at only a slightly higher altitude and sampling similar periods of local time. The present data are, however, free of any altitude dependence, and provide information on longitudinal variations during different seasonal periods than the data of Taylor (1971, 1972). New phenomena associated with the observed longitudinal dependence of the ion composition at 1400 km demonstrate the existence of complex physical processes operative in this region of the ionosphere.

INSTRUMENTATION AND ANALYSIS

The ISIS-II satellite was launched April 1, 1971, into an 88° prograde orbit with an almost constant altitude of 1400 km. The payload included a magnetic sector-field ion mass spectrometer designed to measure concentrations of atmospheric positive ions between 1 and 64 amu. The specific details of this instrument have been reported by son and Hoffman (1973) and Hoffman et al. (1974), and are similar to the descriptions of comparable instruments flown on Explorer XXXI (Hoffman, 1969) and the Atmosphere Explorer (Hoffman et al., 1973) satellites.

A special feature of the ion mass spectrometer onboard ISIS-II is its capability to measure absolute concentrations of the major ionic

species, with, for example, a sensitivity to H^+ and O^+ of 0.1 and 0.5 ions/cm^3, respectively. Absolute measurements are accomplished by in-flight calibration against electron density data from an onboard topside sounder. This particular calibration technique is described by Hoffman (1969) and Hoffman et al. (1974). Its resultant accuracy is considered to be better than $\pm$ 10% in well-behaved regions of the ionosphere, with some degradation in accuracy in the highly-structured polar regions. In the normal mode of operation, the instrument is capable of providing ion densities once every 18 seconds, the nominal satellite spin period. The nearly-circular orbit, $\pm$ 30 km from nominal, of the satellite eliminates all altitude dependence, and provides a global mapping of the latitudinal and longitudinal variations of all of the principal ions for different seasons and local times. The present analysis is, however, restricted to the major ions, H^+, O^+, and He^+ for a specific time of the year.

Data on ion concentrations are discussed in terms of geomagnetic longitude as measured from the geographic meridian through the north magnetic pole, with attention restricted to magnetic dip latitudes between $\pm$ 50 degrees. Due to the nominal 110 minute period of the ISIS-II orbit, differences of about 8 degrees in geographic longitude occur between the extreme northern and southern latitudes considered; the corresponding variations in geomagnetic longitude are, however, unimportant as far as the present analysis is concerned. The geomagnetic longitude and local time to be associated with a particular satellite semi-orbit are those characteristic of the dip equator.

Ion composition data are presented for the two seasonal periods, 23 April - 11 May and 19 Oct - 10 Nov, 1971; these periods are characterized by similar solar declination angles and local times of the satellite

orbits. Unfortunately, this ISIS-II coverage of the equatorial regions was not comprehensive in longitude for any extended period of time. Best low-latitude coverage has existed near 0° geomagnetic longitude over the Americas, with sparse but adequate data near +90° over Europe. Taylor (1971, 1972) has demonstrated that data obtained at different seasons and longitudes can be favorably compared, provided proper consideration is given to the angle, α, between the plane of the dipole equator and the earth-sun line. (This α parameter should be distinguished from the solar declination angle and the angle α^* which are referenced to the geographic equator and to the magnetic dip equator, respectively.) Hence data obtained near 0° geomagnetic longitude in Oct/Nov are essentially equivalent to that at 180° in April/May, and vice versa. Data near these specific longitudes can thus be coordinated to provide a more extensive data base for the two given seasonal periods. Similar relationships are not applicable between the $\pm$90° data because of distortions of the geomagnetic field near +90° from that of a pure dipole (see, e. g., Figure 2 of Brinton et al. (1970)).

To best demonstrate gross variations in global behavior, orbits of ion concentration data are classified into finite regions near 0°, +90°, and 180° geomagnetic longitude, with the major portion of the chosen data falling within $\pm$ 30° of the reference longitude. The nature and sparseness of the -90° data do not warrant its general consideration in this manner. The data presented in the various figures are coded with a notation that refers to the month and the actual geomagnetic longitude of the observation; e.g., A+92 implies data at +92° geomagnetic longitude in April. Further information on a particular satellite orbit can thus be obtained from the summary presented in Table 1. Likewise, the designations of the different longitude sectors are prefixed with A (April/May) or O (Oct/Nov) to indicate the applicable seasonal period. As discussed in the preceding paragraph, data at 0° and 180° geomagnetic

longitudes are relevant, but with different interpretations, to both seasonal periods; hence the general reference to such data is in terms of that longitude associated with April/May. Such "effective" geomagnetic longitudes, abbreviated egmlg, for the Oct/Nov data are obtained by subtracting 180° from the actual geomagnetic longitudes.

The local time coverages of the present data are the 14-17.5 hr period in the afternoon, and 02-05.5 hrs predawn. Although not rigorously correct in all cases, the general term "predawn" has been adopted to characterize the present nighttime data. The local time for any specific orbit can be obtained from Table 1. The seasonal designations "summer" and "winter" also serve to distinguish the two geographic hemispheres, even though the data are strictly applicable for a seasonal period intermediate between equinox and solstice. The related concept of "geomagnetic season" which references the solar ecliptic plane to the geomagnetic equator is of special importance in the interpretation of the present ionospheric data.

The data reported and discussed in this paper have been specially selected to reflect time periods of low magnetic activity. Although the majority of these data in Table 1 reflect k_p levels of 2 or less, the inclusion of selected cases with higher k_p was necessitated by the sparseness of data

in certain longitude regions. There are, in general, no special characteristics of such data that have been attributed to enhanced magnetic activity. An attempt has also been made, where possible, to accentuate data for which no unusual magnetic activity had occurred over the previous 12 hours; the results and conclusions are, therefore, considered to be representative of the normal undisturbed ionosphere.

THE NIGHTTIME IONOSPHERE AT 1400 KM

1. Results from ISIS-II.

The nighttime measurements for the seasonal periods of interest cover predawn local times between 02 and 05.5 hours. Figures 1 and 2 illustrate the general variabilities with longitude of the latitudinal profiles for the major observed nighttime ionic species, H^+ and He^+, respectively; each figure has subdivisions that refer to limited regions near 0° and 180° egmlg, and near +90° geomagnetic longitude in April/May (A+90°) and in Oct/Nov (O+90°). O^+ being a minor ion under predawn conditions at 1400 km, the observed longitudinal variability of its concentration is summarized in Figure 3 with only selected representative satellite orbits.

As H^+ is the dominant nighttime ion at 1400 km for the major portion of the low and mid latitudes, its overall behavior also reflects that of the total ionization. This predawn level of ionization ($\sim 10^4$ ions/cm^3) is comparable to that observed at this same altitude in the afternoon.

(a). H^+.

Figure 1 provides a comparison of the predawn concentrations for H^+ between the different regions of geomagnetic longitude. These H^+ profiles are, in general, fairly symmetric about the dip equator with little

variation over most of the latitude range considered. However, small concentration maxima often appear near the mid latitudes in some of the longitude regions. The winter mid-latitude trough in H^+ extends to lower latitudes in the region near 0° egmlg (Figure 1 (b)), otherwise there is only a slight longitudinal effect with regard to the H^+ profiles and the overall predawn ionization at this altitude.

(b). He^+.

He^+ is usually the ion of second importance in the undisturbed predawn ionosphere at 1400 km, with a clearly-identifiable longitudinal variability in Figure 2:

1. Near 0° egmlg, He^+ has a deep equatorial trough with maxima at the midlatitudes. These curves in Figure 2(b) are reasonably symmetric about the dip equator.
2. The above characteristic equatorial trough is not present in the A+90° data; it is there replaced by a broad deep depression extending to midlatitudes in the winter hemisphere, with a sharp concentration enhancement evident above 40° winter dip latitude.
3. The data near 180° egmlg (Figure 2(d)) resemble to some extent that near A+90°, but with the winter depression somewhat less deep and shifted to lower latitudes.
4. At 0+90°, the He^+ depression extends through both hemispheres to near 40° dip latitude, followed by concentration increases at higher latitudes.

The depletion of light ions in the trough regions above 50° dip latitude (e.g. Taylor and Walsh, 1972) results in especially sharp mid-latitude peaks in nighttime He^+ in the winter hemisphere near A+90° (Figure 2(c)) and in the summer hemisphere near 0+90° (Figure 2(a)). Such peaks are observed in the extension of the given ISIS-II data to the higher latitudes.

(c). O^+.

Because of its status as a relatively minor species during predawn hours at 1400 km, the only ISIS-II data presented for the longitudinal variation of nighttime O^+ are that summarized in Figure 3. An important feature of these observed profiles is the concentration peak at the dip equator. The primary longitudinal variability of O^+ in Figure 3 is reflected in the mid-latitude summer enhancement in the regions near A+90° and 180° egmlg.

(d). Comparison of Relative Behaviors.

The general features of the longitudinal variation of the relative concentrations of H^+, He^+, and O^+ over the latitude range $\pm$ 50° can be obtained through comparisons of the variations of He^+ and O^+ (Figures 2 and 3) with the essentially invariant H^+ concentrations in Figure 1. He^+ is normally the ion second in concentration for predawn at 1400 km, and achieves its greatest magnitude at the higher latitudes before becoming depleted in the polar regions. He^+ and O^+ appear to be anti-correlated in the sense that at low latitudes changes in nighttime O^+ are usually associated with opposite changes in He^+. Large relative changes in the concentrations of He^+ and O^+, in general, reflect only minor unresolved relative changes in the concentrations of H^+; hence correlations between predawn H^+ and either He^+ or O^+ are inconclusive.

2. Comparison with Previous Results.

Limited comparisons are possible between the present nighttime ISIS-II data at 1400 km, and published results from OGO-4 (Chandra et al., 1970) and OGO-6 (Taylor, 1972) near 900 and 1100 km, respectively. However, such OGO-4 data refer to conditions near midnight at equinox, while the

relevant portions of the OGO-6 results are applicable for predawn at equinox and midnight-predawn near solstice. Hence seasonal, altitude and local time differences must be recognized when evaluating comparisons of the present with these previous data. Such factors may, for example, be responsible for the ISIS-II observations of a predawn level of ionization at 1400 km that is somewhat below that suggested by the above lower-altitude measurements. On the positive side, there are several features in the ISIS-II data, such as the mid-latitude enhancements of H^+ at selected longitudes (Figure 1), that are also recognized in the earlier data.

The equatorial He^+ trough that was discussed with regard to Figure 2 is also a characteristic feature of the above-cited OGO data. Mid-latitude depressions of He^+ are likewise observed in the predawn OGO-6 data (Taylor, 1972), where they are either present in both hemispheres or favor the hemisphere approaching summer. The existence of an opposite seasonal effect noted in Figures 2(c) and 2(d) of the ISIS-II data is not apparent in the data of Taylor (1972).

The large diurnal variations in O^+ at 1400 km (compare Figure 3 with Figure 4 to follow) result in a strong dependence of the magnitude of the nighttime equatorial peak on local time. The observed concentration level (Figure 3) is comparable to that of Taylor (1972) at predawn, but the corresponding midnight data of Chandra et al. (1970) show this equatorial O^+ maximum to be over an order of magnitude larger and intermediate between H^+ and He^+. The mid-latitude enhancement of nighttime O^+ at selected longitudes (Figure 3) is also present in the equinox data of Taylor (1972) and Chandra et al. (1970), being illustrated at negative geomagnetic longitudes (where there is no ISIS-II data) for the hemisphere

approaching summer. The observation of these O^+ enhancements near local midnight at equinox (Chandra et al., 1970) eliminates presunrise effects as their primary source.

The apparent anti-correlation between the low-latitude behaviors of nighttime O^+ and He^+, that was mentioned in part 1 (b) of this section, has also been observed in comparisons of the present ISIS-II profiles both with those obtained closer to local midnight and with those obtained during magnetic disturbances; in such studies any equatorial increases of O^+ are well correlated with simultaneous depletions in He^+. Such a relationship between He^+ and O^+, also observed at lower altitudes, has been discussed by Chandra et al. (1970) who consider various charge transfer reactions leading to O^+ and N^+ as possible loss mechanisms for He^+. However, little laboratory information is available on the relevant reaction rates. Ionospheric dynamics could also play a role in this important, but yet unexplained, feature of the topside ion distribution.

THE DAYTIME IONOSPHERE AT 1400 KM

1. Results from ISIS-II.

The daytime ion concentration data to be presented from ISIS-II cover the local time period between 14 and 17.5 hours. These data show the total ion concentration in the afternoon near 1400 km to be comparable to that observed at predawn, with a magnitude near 10^4 ions/cm^3. A unique feature of the ISIS-II results is the existence of two distinct types of daytime ionosphere at 1400 km at this particular time of the year. One category was present near 0° egmlg; a distinctively different ionospheric behavior has been observed in the April/May longitude region near +90° extending to 180°. Differences between these contrasting

ionospheres are most apparent in the low-latitude profiles of O^+ and He^+.

A summary is presented of the observed variations with longitude of the latitude concentration profiles for the three daytime constituents, O^+, H^+ and He^+. Special phenomena associated with the region near 180° egmlg warrant separate discussion in the next section.

(a). O^+.

Although a minor ion at night, O^+ is a major and in places the dominant ion in the afternoon at 1400 km. The longitude and latitude variabilities of this important F-region ion are illustrated in Figure 4. Near 0° egmlg (Figure 4(b)), there is a broad plateau of O^+ in the summer hemisphere followed by a deep depression in winter. O^+ is the dominant ion at summer latitudes, but is secondary to H^+ in the winter hemisphere at this altitude.

The characteristics of O^+ near 0+90° are difficult to evaluate because of incomplete equatorial coverage by the satellite. However, the portions of orbits displayed in Figure 4(a) suggest such behavior to be similar to that observed near 0° egmlg (Figure 4(b)). This property is especially noticeable with regard to the winter depression at mid latitudes.

In contrast, the variations with latitude of the O^+ concentrations near A+90° (Figure 4(c)) are distinctively different from those described above. These 90° profiles are more regular, with the winter depressions replaced by more gradual declines in concentration.

(b). H^+.

Daytime concentration profiles for H^+ from ISIS-II are summarized in Figure 5; this latitudinal behavior of H^+ is, in some respects, opposite to that of O^+. Near 0° egmlg (Figure 5(b)), H^+ tends toward a maximum and is the most abundant ion in the winter hemisphere.

Its concentration remains reasonably constant over a considerable range of summer latitudes, but at a magnitude less than 1/2 that of O^+. By comparison, the H^+ profiles near A+90° (Figure 5(c)) have broad maxima at, and are symmetric about, the dip equator, and do not exhibit the above summer plateaus. In general, the H^+ equatorial concentrations are larger, and the summer mid-latitude concentrations smaller, near A+90° than at 0° egmlg. The nature of the available H^+ data in the 0+90° region (Figure 5(a)) precludes their unique categorization in terms of the other longitude regions. In conclusion, there are observable differences, especially at low latitudes, in the behavior of H^+ between the different longitude regions, although these differences are not as pronounced as those discussed for O^+.

(c). He^+.

The most distinctive feature of the present daytime He^+ data at 1400 km is the deep equatorial trough observed near 0° egmlg (Figure 6(b)). The associated winter He^+ maximum observed in this longitude region is also slightly enhanced over the companion summer maximum. Mid-latitude concentrations of He^+ near 0+90° (Figure 6(a)) possess features that are strongly suggestive of similar latitudinal profiles in this region.

A special ionospheric behavior near A+90° is also evident in the He^+ data (Figure 6(c)). The He^+ equatorial trough observed at other longitudes is completely absent at A+90°, and is, in fact, replaced by a symmetric equatorial bulge. The presence or absence of the equatorial He^+ trough is a convenient way to distinguish the two alternative types of daytime ionospheric behavior observed at 1400 km for this time of the year.

(d). Comparison of Relative Behaviors.

Differences between the two alternative types of daytime ionosphere observed at 1400 km are more apparent in the relative behaviors of the separate ion profiles as illustrated in Figure 7. Near 0° egmlg (Figure 7(b)), O^+ is the most abundant summer ion, with H^+ becoming dominant in the winter hemisphere. In fact, He^+ at times actually exceeds O^+ in concentration at selected latitudes. This is the same longitude region where at 900 km (Taylor, 1971) the daytime H^+ concentrations become comparable in magnitude to the otherwise dominant O^+ concentrations and He^+ exceeds H^+, over limited but not necessarily overlapping, ranges of winter latitude.

These general features near 0° egmlg appear to be also present at 0+90°, and, in addition, are recognized in parts of the 180° egmlg data discussed in the next section. In contrast, at A+90° the H^+ peaks are shifted toward the equator and H^+ remains the most abundant ion farther into the summer hemisphere. The He^+ concentrations are never greater than those of O^+ in this latter longitude region. Furthermore, the H^+ and He^+ concentrations near A+90° vary in a similar manner with latitude, a property not as apparent in the other longitude regions. The anti-correlation between He^+ and O^+, discussed relative to the nighttime data, also appears to be present in Figures 7(a) and 7(b), but is less well-defined in Figure 7(c).

The above features in the ISIS-II data provide strong evidence of the distinctive differences between the daytime ionospheres near 0° egmlg and A+90° in the April/May seasonal period. The type of ionosphere described near 0° egmlg is to be referenced as S-type, as its characteristics have been observed at lower altitudes nearer to solstice (Taylor,1971).

In a similar manner, those features observed with ISIS-II in the region near A+90° are to be labelled E-type since they are postulated to be more representative of conditions near equinox. The basis for such a classification is further discussed in the next section.

2. Comparison with Previous Results.

Comparisons are available between the ISIS-II afternoon data and that reported from OGO-4 by Chandra et al. (1970) for morning in late October and by Taylor (1971) for noon in late May and late afternoon near solstice, and from OGO-6 (Taylor, 1972) in the late afternoon near equinox. Seasonal, altitude and local time differences are thus also involved in these comparisons. The data of Chandra et al. (1970) indicate O^+ to be the most abundant daytime ion near 900 km, at concentrations ($\sim 10^5$ ions/cm^3) that are roughly 10 times the night-time level of ionization (light ions) observed at this same altitude. Such general diurnal behavior is also noted in the OGO-6 equinox data (Figures 5 and 6 of Taylor (1972)), with the late afternoon O^+ concentrations achieving levels in excess of 5×10^4 ions/cm^3 above 900 km. In contrast to these previous results, the ISIS-II data in the afternoon show the total ion concentration near 1400 km to be comparable to that observed at predawn, with a magnitude near 10^4 ions/cm^3. Furthermore, as demonstrated by both the present data and that of Taylor (1971), the daytime dominance of O^+ at these altitudes is definitely restricted in both latitude and longitude. Seasonal, longitudinal, and local time variations between the various sets of measurements probably contribute more to the above differences than does an altitude effect alone.

An important characteristic of the OGO-4 data (late May) of Taylor (1971) is the existence of a seasonal asymmetry at all longitudes in the daytime O^+ concentrations that favors enhancement in the summer hemisphere. This property is also present in the ISIS-II data for the longitude regions exhibited in Figure 4. However, Chandra et al. (1970) in late October observe near -30° egmlg a more

gradual latitudinal decline than that shown for 0° egmlg in Figure 4(b), while Taylor (1971) reports the O^+ concentration in late May at these same longitudes to decrease several orders of magnitude between the summer and winter hemispheres. Hence, for this particular region near 0° egmlg, those O^+ concentration profiles observed closer to solstice possess much greater seasonal asymmetry than corresponding data taken nearer to equinox. This strong seasonal variability for O^+ is a specific example of the more general dependence of the topside ion profiles on the orientation of the geomagnetic field relative to the sun (i.e., on the α parameter of Taylor (1971)); however, the precise nature of this dependence remains undefined. Whatever its form, such a relationship can also result in a significant longitudinal variation in the daytime O^+ data at certain times of the year. This latter effect is quite discernible in the ISIS-II data where the summer enhancements of O^+ in Figure 4 contrast sharply with an almost-negligible seasonal behavior discussed in the next section relative to data near 180° egmlg.

If one excludes the region near 0° egmlg, the lower-altitude noontime H^+ data of Taylor (1971) from OGO-4 have the same general symmetry properties with respect to the magnetic equator as those shown in Figure 5(c). These properties are also noted in the selected daytime H^+ profile discussed with regard to the OGO-6 data (Figure 5 of Taylor (1972)) at 1100 km near the spring equinox. The principal difference between the above OGO-4 and the present sets of daytime H^+ data occurs in the longitude region near 0° egmlg, where the broad latitudinal profiles in Figure 5 (b) give no indication of the mid-latitude winter depletions observed by Taylor (1971).

The equatorial trough and relative winter enhancement in the daytime He^+ concentrations are special characteristics of the noon data near 900 km

discussed by Taylor (1971). Such data, however, indicate these features to be present at all longitudes. Hence the ISIS-II observations for He^+ (Figure 6(c)) differ significantly from the corresponding May data of Taylor (1971) near +90° geomagnetic latitude. However the measurements of Taylor (1971) refer to a seasonal period closer to solstice than those presented from ISIS-II, and these contrasting behaviors of He^+ near A+90° could arise from the same seasonal effects that are responsible for those variations discussed in the next section for the region near 180° egmlg.

VARIATIONS IN THE DAYTIME IONOSPHERE NEAR 180° EGMLG

As discussed in part 1 of the previous section, the observed daytime ionosphere near A+90° (denoted as E-type) is distinctively different from that at 0° egmlg (S-type). Daytime data obtained in the vicinity of 180° egmlg indicate features that are associated with both types of ionosphere. The existence of such contrasting behavior can be established through the data summarized in Figure 8 for O^+ and He^+, species for which the differences are the most apparent. A distinguishing feature of the S-type of He^+ profiles in Figure 8(a) is the presence of an equatorial trough similar to that observed near 0° egmlg in Figure 6(b). Alternatively, the symmetric equatorial maxima found near A+90° in Figure 6(c) suggest the He^+ profiles of Figure 8(b) to belong to the E category. These same classifications are also applicable to the O^+ profiles in Figure 8, with, however, some minor modifications. An E-type of O^+ profile defined according to Figure 4(c) decreases at a steady rate from the summer to the winter hemisphere, while the corresponding curves in Figure 8(d) show an opposite seasonal effect with indications of a slight equatorial

depression. However, the O^+ curves labelled S-type in Figure 8(c) do exhibit the formation of equatorial maxima that should develop to the sharp equatorial gradients and summer plateaus observed in Figure 4(b) as the season evolves toward solstice. Such O^+ peak development is well correlated with the formation of the daytime He^+ equatorial troughs, as demonstrated through the profiles of Figure 8, and of Figures 9 and 10 to follow. Although the features that distinguish the basic E- and S-types of daytime ionosphere are weakly defined in the 180° egmlg data, the concurrent consideration of both O^+ and He^+ behaviors for a particular orbit reduces any ambiguity in its classification. The particular presentation in Figure 8 demonstrates that the given classification scheme is meaningful for the 180° egmlg data as a whole.

Portions of the data in Figure 8 possess distinct longitudinal and time variations that warrant special attention. Figure 9 compares profiles of O^+ and He^+ between successive satellite orbits, for two separate days. On each of these days, the existence of an S-type of ionosphere at negative egmlg near 180° (the solid curves) is readily distinguishable from the E-type (dashed curves) observed one orbit later at positive egmlg. Figure 10 presents two sets of data at approximately the same longitude, but separated by a time period of about a week. The particular orbits selected for Figures 9 and 10 are representative of other examples in the data. Such figures demonstrate that significant changes in ionospheric characteristics at low latitudes are possible between successive orbits, or within a short seasonal time span, for these longitudes and seasonal periods.

The daytime data near 180° egmlg have also been analyzed with regard to a possible seasonal effect, as reflected in the magnitude of the solar declination angle. The results utilizing a major portion of the available relevant data are illustrated in Figure 11. Each dot and open circle represent a value of the solar angle and associated longitude at which an E-type of ionosphere has been observed; the crosses denote similar parameters for the S-type. The points for each such category tend to be confined to distinct areas of the figure. Observation of an E-type of ionosphere is favored at positive egmlg, and for the smaller solar angles; as the solar angle increases, a region of S-type features develops at negative egmlg and expands toward positive egmlg. Two special observations, accentuated with arrows, prevent the location of the corresponding transition region from being linear (i.e., lie within the dashed band) with solar declination angle. Hence, although there are definite indications of a general dependence of this ionospheric behavior on solar declination angle, the presence of these two well-defined S-type profiles (coded A+170 and N-6 in Figure 8) at positive egmlg suggests that other shorter-term processes may also be operative.

As described in the next section, the ionospheric characteristics near +90° and 180° geomagnetic longitudes are expected to be somewhat similar because of distortions in the geomagnetic field. The E-type of behavior noted near 180° egmlg (Figure 8) can thus be directly related to that observed in the A+90° region (Figures 4(c) and 6(c)). Although rigorous conclusions are hindered by the lack of satellite data in the -90° geomagnetic longitude region, the observations at 1400 km are

consistent with the following interpretation. During late April and October, the daytime ionosphere near 180° egmlg is basically E-type with the E/S transition region at large negative egmlg. As the season evolves toward middle May or November, the daytime ionospheric features near 180° egmlg become more characteristic of the S-type. Such a trend is supported by Taylor (1971), whose data exhibit S-type properties at all longitudes in late May. These seasonal changes are, however, small in magnitude compared to the diurnal O^+ variations at this altitude, and other processes (e.g. magnetic disturbances) may cause significant short-term deviations from this generalized behavior.

DISCUSSION

This presentation of data from ISIS-II satellite at 1400 km has emphasized longitudinal variations of the principal topside ions at low and mid latitudes. There are several general features of the observed variations that demonstrate in a unique manner the important role of the geomagnetic field and its orientation relative to the sun. This discussion is directed primarily toward O^+ and He^+, species for which such longitudinal variations are the most pronounced.

1. A Generalized Solar-Geomagnetic Seasonal Dependence.

Taylor (1971, 1972) has described the solar influence over the topside ion distributions in terms of the angle, α, between the earth-sun line and the magnetic dipole equator. The latter simple model of

the geomagnetic field is reliable at low latitudes near 0° and 180° geomagnetic longitudes. Hence we have utilized the general conclusions of Taylor (1971, 1972) to coordinate data from two separate seasonal periods into an enlarged data base near these specific longitudes. Limited comparisons are available within Figures 2(b), 4(b), and 6(b), respectively, between April/May data near 0° and Oct/Nov data near 180° geomagnetic longitude. Comparable information can be obtained from Figures 2(d) and 8 relative to April/May data near 180° and Oct/Nov data near 0° geomagnetic longitude. The general similarities of the concentration profiles within each of these figures are consistent with predictions from the dipole model of Taylor (1971, 1972).

There are, in addition, more subtle comparisons available in the ISIS-II data that lead to an extension and generalization of the above α-angle concept. The dipole field model of Taylor (1971, 1972) would suggest, for example, the equivalence of the +90° (April/May) and -90° (Oct/Nov) geomagnetic longitude regions. However, distortions of the true geomagnetic field in the +90° geomagnetic longitude region, as illustrated in Figure 2 of Brinton, et al. (1970), are sufficient to preclude any positive conclusions from such a comparison for the actual data. In fact, the magnetic dip equator near +90° lies as far north geographically as it does at 180° geomagnetic longitude. Since the ISIS-II data are referenced to the magnetic dip equator, there should exist favorable comparisons between observed ion concentration profiles at +90° and 180° geomagnetic longitudes in any given seasonal period. Hence, features of the data near A+90° should be similar to those near 180° egmlg. Such properties in the night-time data are confirmed through comparisons of Figures 2(c) and 2(d) for He^+, and of the O^+ profiles labelled M+76 and

N-13 in Figure 3. As discussed in the previous section, portions of the daytime data at 180° egmlg (Figures 8(b) and 8(d)) also have properties identifiable with curves in Figures 4(c) and 6(c).

An additional relevant comparison is suggested by this generalization. Data at 90° geomagnetic longitude in Oct/Nov, being comparable to that at 180° (Oct/Nov), should possess properties that approximate the features near 0° (April/May). That is, there should be general similarities between the ion profiles of the 0+90° and 0° egmlg regions. The night-time O^+ curves, labelled M-6, 0+71 and N+102, in Figure 3 are indeed consistent with such a relationship; the same is true in the daytime data for the O^+ profiles in Figures 4(a) and 4(b), and for the He^+ profiles in Figures 6(a) and 6(b). Although appreciable differences are noted between the night-time He^+ curves in Figures 2(a) and 2(b), both such sets of data do possess greater equatorial symmetry than do the He^+ profiles at other longitudes.

The ISIS-II data thus provide support to the conclusions of Taylor (1971, 1972) in those longitude regions where the dipole model is a valid approximation to the geomagnetic field. The data also suggest a general extension of such concepts to regions where field distortions occur. The important quantity for the favorable comparison of ionospheric behavior between different seasonal periods is thus an effective α^* parameter which references the earth-sun line to the localized magnetic dip equator. Observations by ISIS-II thus confirm the strong solar-geomagnetic seasonal control over the topside ionization, even at night.

2. The Daytime Ionosphere.

Important questions remain concerning the nature of those physical processes responsible for the daytime features that distinguish the A+90° and 0° egmlg regions. Such features relate primarily to the O^+ concentration gradient at low latitudes, and to the presence or absence of the He^+ equatorial trough. The ionospheric variations observed near 180° egmlg are probably special manifestations of these same physical processes. This discussion emphasizes solar-induced effects on O^+ variations at low latitudes; longitudinal variations of He^+ are assumed to be a consequence of the normally observed, but still unexplained, relationship of these concentrations with O^+ at 1400 km.

The solar declination angle, ψ, increased between about 9.5 to 17.5 degrees throughout the seasonal periods of the composite data base; during such an interval the daytime northern and southern geomagnetic hemispheres in the region near 180° egmlg achieved a high degree of symmetry with respect to the ecliptic plane. This condition is illustrated in Figure 12 for the special case of local noon at 180° (April/May). When the sun is in the direction indicated, such symmetry is attained when ψ is equal to θ_o ($\sim$ 11.4°), the angular difference between the geomagnetic and geodetic poles. For $\psi < \theta_o$, the ionospheric seasonal characteristics at these longitudes favor northern winter and southern summer. The situation here reverses for $\psi > \theta_o$, as the seasonal asymmetry with respect to the magnetic equator becomes consistent with that at other longitudes. Because of the magnetic field geometry, a similar transition between "geomagnetic seasons" should occur almost concurrently near A+90°. An effective ionospheric season of near-equinox thus exists in both the

A+90° and 180° egmlg regions during the reported period of ISIS-II observations; hence differences between the northern and southern daytime ionospheres at these longitudes should be especially sensitive to solar-induced processes during such a seasonal interval.

Solar influence on ionospheric behavior can be exerted directly via the production and subsequent redistribution of ionization, or indirectly through the stimulation of comparable processes in the background neutral atmosphere. The resultant effects of both mechanisms should exhibit similar dependences on solar zenith angle, and hence on season; the basic distinction is the strength of the fundamental processes involved. Brinton et al. (1970) have investigated the effects of solar-induced atmospheric winds relative to ion concentration measurements between 1000 and 2000 km from Explorer 32 satellite. Such data, obtained near mid-day between June and September, indicate a strong seasonal asymmetry in O^+ between -30° and +20° geomagnetic longitude, as compared with nearly symmetrical profiles in the +70° to +120° and the -110° to -170° regions. A theoretical model, applicable for 0° and 180° geomagnetic longitudes at geographic equinox, served to demonstrate that meridional winds in the neutral atmosphere were capable of producing the observed longitudinal O^+ variations. Such winds may also be a factor in explaining similar effects observed with ISIS-II.

Solar-induced changes in the rate of O^+ production and associated redistribution provide an additional mechanism for producing the observed daytime longitudinal variations. The ultimate role of solar radiation in this regard must be considered in terms of its effects at lower

altitudes near the F_2 peak where the major portion of the overall O^+ ionization is produced, and from where the resultant effects are propagated to the altitude of observation. The O^+ concentrations at 1400 km are especially sensitive to such photoionization and transport processes, as evidenced by their large diurnal variations. Seasonal and longitudinal effects are essentially perturbations to these large diurnal O^+ variations; hence direct solar ionization processes should also be capable of producing the observed daytime ionospheric variations.

The daytime ISIS-II data near A+90° provide no indications of variations comparable to those discussed near 180° egmlg, even for the later portion of the April/May seasonal period. Hence differences persist between these two longitude regions, despite similarity in the geographic latitudes of their respective magnetic equators. Such effects remain secondary to the general seasonal trend, but could be of the same order as the irregularity in behavior noted in Figure 11. A better treatment of the true geomagnetic field configuration and a consideration of its east-west geographic components could provide an explanation for these higher order effects.

SUMMARY

In summary, absolute concentrations are reported for the principal ions near 1400 km at low and mid latitudes from the ion mass spectrometer onboard the ISIS-II satellite. Data are discussed for afternoon (14-17.5 hr) and predawn (02-05.5 hr) local times during April/May and Oct/Nov, 1971. Satellite coverage has been sufficient to allow comparisons of the latitudinal behaviors of these ions between the 0°, +90°, and 180° geomagnetic longitude regions for both such seasonal periods. Many features of these variations are quite different from those reported by other investigators.

The overall predawn level of ionization at 1400 km is found comparable to that observed in the afternoon. The dominant nighttime ion, H^+, exhibits little horizontal variability over the major portion of the low and mid latitudes. However, the seasonal asymmetry of O^+ is strongly dependent on longitude, and the well-defined equatorial trough in He^+ present in certain longitude regions develops at other longitudes into broad depressions that extend well into the middle latitudes.

The observed daytime latitudinal profiles of ion concentration also exhibit a complex longitudinal behavior, with O^+ and H^+ competing for dominance over the given latitude range. Certain longitude regions are distinguished by broad summer plateaus of O^+, separated by sharp equatorial gradients from concentration depressions in the winter hemisphere. H^+ has a slight enhancement and becomes the dominant daytime ion at the winter latitudes. The equatorial He^+ trough is also a characteristic feature at these longitudes. In contrast, an extended region of longitude has been observed over which the seasonal O^+ asymmetry is much less pronounced, and where both H^+ and He^+ exhibit symmetric concentration peaks near the

magnetic dip equator. These behaviors are inferred to reflect two distinct (S and E) classes of low-latitude daytime ionosphere at this altitude and season. Both types of features are recognized in data applicable to 180° (April/May) geomagnetic longitude, with indications of a general longitudinal and seasonal dependence. Direct solar photoionization and transfer processes, as well as interaction of the ionosphere with neutral atmospheric winds, are considered capable of providing the basic source mechanism for the observed daytime longitudinal effects.

The ISIS-II data confirm the strong solar-geomagnetic seasonal control (Taylor; 1971, 1972) over the topside ion distribution. This property is further demonstrated by improved comparisons of ion profiles between different longitudes and seasons that result when the solar direction is referenced to the magnetic dip equator. However, a more-refined model of ionospheric chemistry and dynamics, based on a more-rigorous representation of the geomagnetic field and including such minor species as He^+, remains a necessary prerequisite for complete understanding of these ISIS-II observations.

ACKNOWLEDGMENTS

The authors gratefully acknowledge the efforts of W. H. Dodson and J. S. Donaldson in the reduction of the satellite data. This work was supported by The National Aeronautics and Space Administration grant NGR44-004-030 and contract NAS5-11003.

REFERENCES

Brinton, H. C., H. G. Mayr, R. A. Pickett, and H. A. Taylor, Jr., The effect of atmospheric winds on the O^+ -H^+ transition level, Space Res., 10, 652-662, 1970.

Chandra, S., B. E. Troy, Jr., J. L. Donley, and R. E. Bourdeau, OGO 4 observations of ion composition and temperatures in the topside ionosphere, J. Geophys. Res., 75, 3867-3878, 1970.

Dodson, W. H., and J. H. Hoffman, Ion composition measurements from ISIS-II satellite (abstract), EOS Trans. AGU, 54, 384, 1973.

Hoffman, J. H., Ion mass spectrometer on Explorer XXXI satellite, Proc. IEEE, 57, 1063-1067, 1969.

Hoffman, J. H., W. H. Dodson, C. R. Lippincott, and H. D. Hammack, Initial ion composition results from the ISIS-II satellite, to be published, 1974.

Hoffman, J. H., W. B. Hanson, C. R. Lippincott, and E. E. Ferguson, The magnetic ion-mass spectrometer on Atmosphere Explorer, Radio Sci., 8, 315-322, 1973.

Taylor, H. A., Jr., Evidence of solar geomagnetic seasonal control of the topside ionosphere, Planet. Space Sci., 19, 77-93, 1971.

Taylor, H. A., Jr., Observed solar geomagnetic control of the ionosphere: implications for reference ionospheres, Space Res., 12, 1275-1290, 1972.

Taylor, H. A., Jr., H. G. Mayr, and H. C. Brinton, Observations of hydrogen and helium ions during a period of rising solar activity, Space Res., 10, 663-678, 1970.

Taylor, H. A., Jr., and W. J. Walsh, The light-ion trough, the main trough, and the plasmapause, J. Geophys. Res., 77, 6716-6723, 1972.

Figure Captions

Figure 1. Latitudinal profiles of the predawn H^+ concentration (02-05.5 hr local time) at 1400 km. Regions of geomagnetic longitude are prefixed with A or O to denote the respective April/May or Oct/Nov seasonal period. Individual curves are referenced to orbital data in Table 1.

Figure 2. Latitudinal profiles of the predawn He^+ concentration (02-05.5 hr local time) at 1400 km. Regions of geomagnetic longitude are prefixed with A or O to denote the respective April/May or Oct/Nov seasonal period. Individual curves are referenced to orbital data in Table 1.

Figure 3. Variations with latitude and longitude of the predawn O^+ concentration (02-05.5 hr local time) at 1400 km. Individual curves are referenced to orbital data in Table 1. Regions of geomagnetic longitude are identified as follows: ____, 0° egmlg; ...., 180° egmlg; ---; A+90°; -·-·-, O+90°. The first three regions are referenced to the April/May, and the final to the Oct/Nov, seasonal period.

Figure 4. Latitudinal profiles of the afternoon O^+ concentration (14-17.5 hr local time) at 1400 km. Regions of geomagnetic longitude are prefixed with A or O to denote the respective April/May or Oct/Nov seasonal period. Individual curves are referenced to orbital data in Table 1.

Figure 5. Latitudinal profiles of the afternoon H^+ concentration (14-17.5 hr local time) at 1400 km. Regions of geomagnetic longitude are prefixed with A or O to denote the respective April/May or Oct/Nov seasonal period. Individual curves are referenced to orbital data in Table 1.

Figure 6. Latitudinal profiles of the afternoon He^+ concentration (14-17.5 hr local time) at 1400 km. Regions of geomagnetic longitude are prefixed with A or O to denote the respective April/May or Oct/Nov seasonal period. Individual curves are referenced to orbital data in Table 1.

Figure 7. Comparison of the afternoon (14-17.5 hr local time) relative concentrations of the major ions at 1400 km in different longitude regions. The A and O prefixes to the geomagnetic longitude regions refer to the April/May and Oct/Nov seasonal periods, respectively. Satellite orbits are representative of those illustrated in Figures 4, 5, and 6, and are referenced to orbital data in Table 1.

Figure 8. Contrasting types of afternoon (14-17.5 hr local time) concentration profiles for O^+ and He^+ at 1400 km observed in the geomagnetic longitude sector equivalent to 180° (April/May). Profiles are categorized as S- or E- type to indicate similarities to data at A+0° or A+90°, respectively, in Figures 4 and 6. Individual curves are referenced to orbital data in Table 1.

Figure 9. Contrasting types of afternoon ion profiles (14-15 hr local time) at 1400 km observed on successive satellite orbits in the geomagnetic longitude sector equivalent to 180°(April/May). The solid and dashed curves reflect the S- and E- types of behavior, respectively, as illustrated in Figure 8, and are referenced to orbital data in Table 1.

Figure 10. Contrasting types of afternoon ion profiles (14.5-15.2 hr local time) at 1400 km observed about a week apart near a selected longitude in the geomagnetic longitude sector equivalent to

(Figure 10.) 180° (April/May). The solid and dashed curves reflect the S- and E- types of behavior, respectively, as illustrated in Figure 8, and are referenced to orbital data in Table 1.

Figure 11. Effect of the solar declination angle on the nature of the afternoon ionosphere at 1400 km in the geomagnetic longitude sector equivalent to 180° (April/May), i.e., near 180° effective geomagnetic longitude. Data points represented by o and ⊗ are supported by profiles in Figure 8, with orbital data in Table 1.

Figure 12. Special geometry for the geomagnetic dipole equator and the solar ecliptic plane during the seasonal periods of the reported observations. When $\psi \sim \theta_o$, the solar ecliptic becomes a plane of symmetry for the northern and southern geomagnetic hemispheres near 180° (April/May) at local

TABLE 1. ISIS-II Satellite Orbit Parameters

Code	Day, 1971	Local Time,* Hr:Min	Orbit	k_p	$k_p(-12)$†	Geomagnetic Dipole Longitude,†* deg	Egmlg,§* deg
A+104	26 April	05:00	316	1-	1-	+104	
A-156	26 April	05:00	325	1o	2+	-156	-156
A+61	30 April	04:50	368	3-	4-	+61	
M+76	4 May	04:30	418	3+	4-	+76	
M-6	9 May	04:00	484	2+	3o	-6	-6
M-150	9 May	04:00	490	3-	3-	-150	-150
M+98	10 May	04:00	493	4-	4-	+98	
M-16	10 May	04:00	497	2-	4-	-16	-16
O+55	19 Oct	03:50	2547	0+	1o	+55	
O-3	19 Oct	03:50	2549	1-	1o	-3	+177
O+99	23 Oct	03:30	2596	0+	3o	+99	
O+71	23 Oct	03:30	2597	0+	3o	+71	
O+64	26 Oct	03:20	2635	0o	2o	+64	
O+7	26 Oct	03:20	2637	0o	2o	+7	-173
O-159	31 Oct	03:00	2706	2o	2o	-159	+21
N+102	5 Nov	02:30	2760	1o	2-	+102	
N+75	5 Nov	02:30	2761	1o	2-	+75	
N-13	5 Nov	02:30	2764	1o	2-	-13	+167
A+103	23 April	17:20	285	2-	3o	+103	
A+75	23 April	17:20	286	2-	3o	+75	
A+3	27 April	17:00	339	2o	3-	+3	+3
A+170	30 April	16:40	371	1+	4-	+170	+170
M+75	1 May	16:40	387	1+	3-	+75	
M+70	4 May	16:30	425	1o	3+	+70	
M+64	10 May	16:00	501	2-	3+	+64	
M+5	10 May	16:00	503	2+	3o	+5	+5
M+167	11 May	15:50	510	0+	3-	+167	+167
O+80	19 Oct	15:50	2553	0+	1-	+80	
O-7	27 Oct	15:10	2656	1-	1-	-7	+173
O+7	31 Oct	15:00	2706	1+	2o	+7	-173
N-147	2 Nov	14:50	2724	0o	1o	-147	+33
N+14	2 Nov	14:50	2731	1o	1o	+14	-166
N-14	2 Nov	14:50	2732	2-	2-	-14	+166
N-6	4 Nov	14:30	2757	2-	2-	-6	+174
N+97	5 Nov	14:30	2766	2-	2-	+97	
N+11	5 Nov	14:30	2769	1o	2-	+11	-169

(Continued on following page)

TABLE 1. (Continued) ISIS-II Satellite Orbit Parameters

Code	Day, 1971	Local Time,* Hr:Min	Orbit	k_p	$k_p(-12)$†	Geomagnetic Dipole Longitude,‡* deg	Egmlg,§* deg
N+18	7 Nov	14:20	2794	1+	3+	+18	-162
N-10	7 Nov	14:20	2795	0o	3-	-10	+170
N-150	10 Nov	14:10	2825	1+	1+	-150	+30
N+100	10 Nov	14:10	2829	0+	1+	+100	
N+72	10 Nov	14:10	2831	1-	1+	+72	
N+15	10 Nov	14:10	2832	2-	2-	+15	-165
N-13	10 Nov	14:10	2833	2o	2o	-13	+167

* These parameters refer to the satellite crossing of the dip equator.

† The maximum value of k_p during the previous 12 hours.

‡ As measured from the geodetic meridian through the north geomagnetic pole.

§ The "effective" geomagnetic longitude, for data near 0° and 180° geomagnetic longitude, as would correspond to the April-May seasonal period.

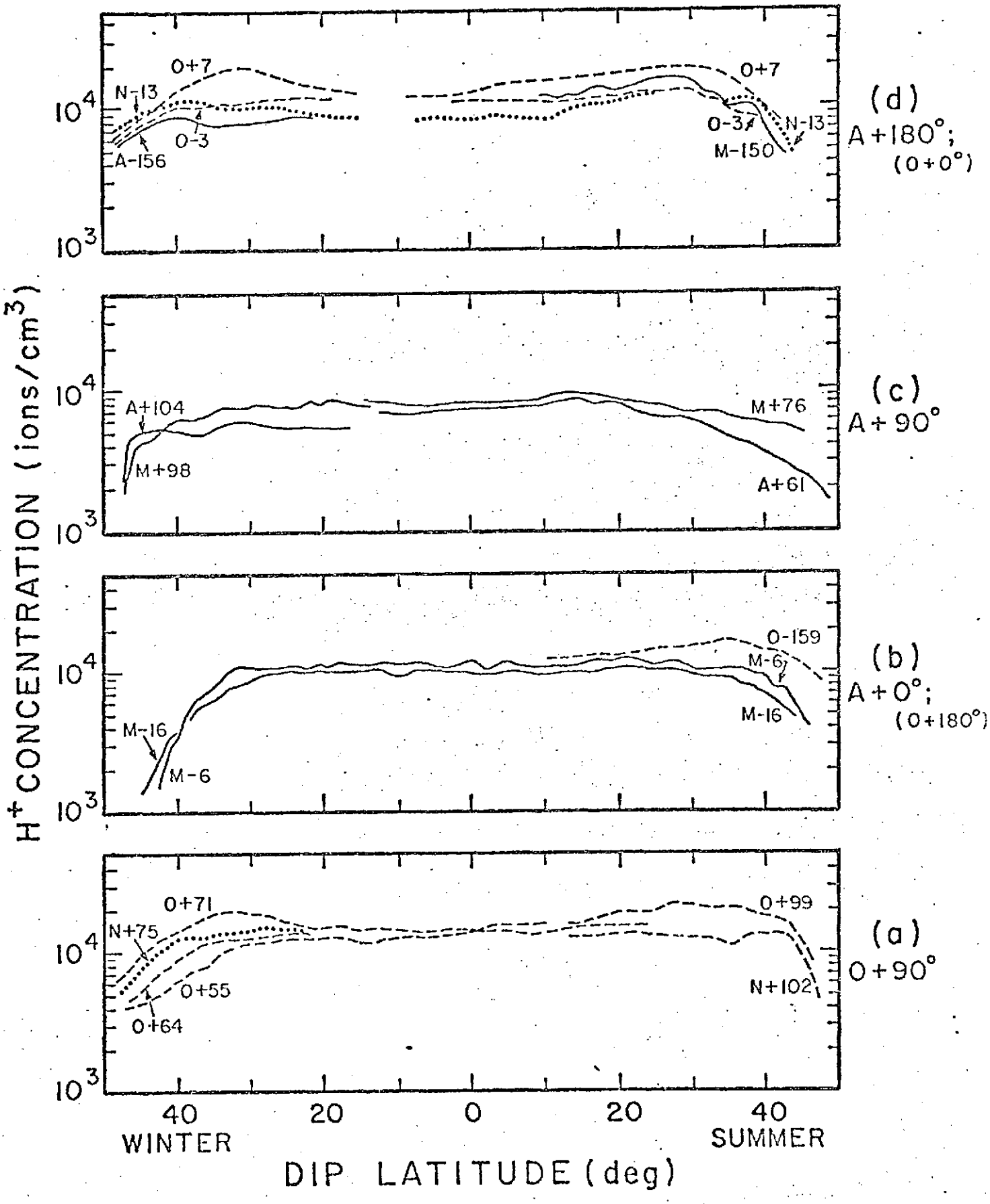
H+ CONCENTRATION (ions/cm3)
10^4
10^3
0+7
N-13
0-3
A-156
0+7
0-3
N-13
M-150
(d)
A+180°;
(0+0°)
A+104
M+98
M+76
A+61
(c)
A+90°
0-159
M-6
M-16
M-16
M-6
(b)
A+0°;
(0+180°)
0+71
N+75
0+55
0+64
0+99
N+102
(a)
0+90°
40
20
0
20
40
WINTER
SUMMER
DIP LATITUDE (deg)

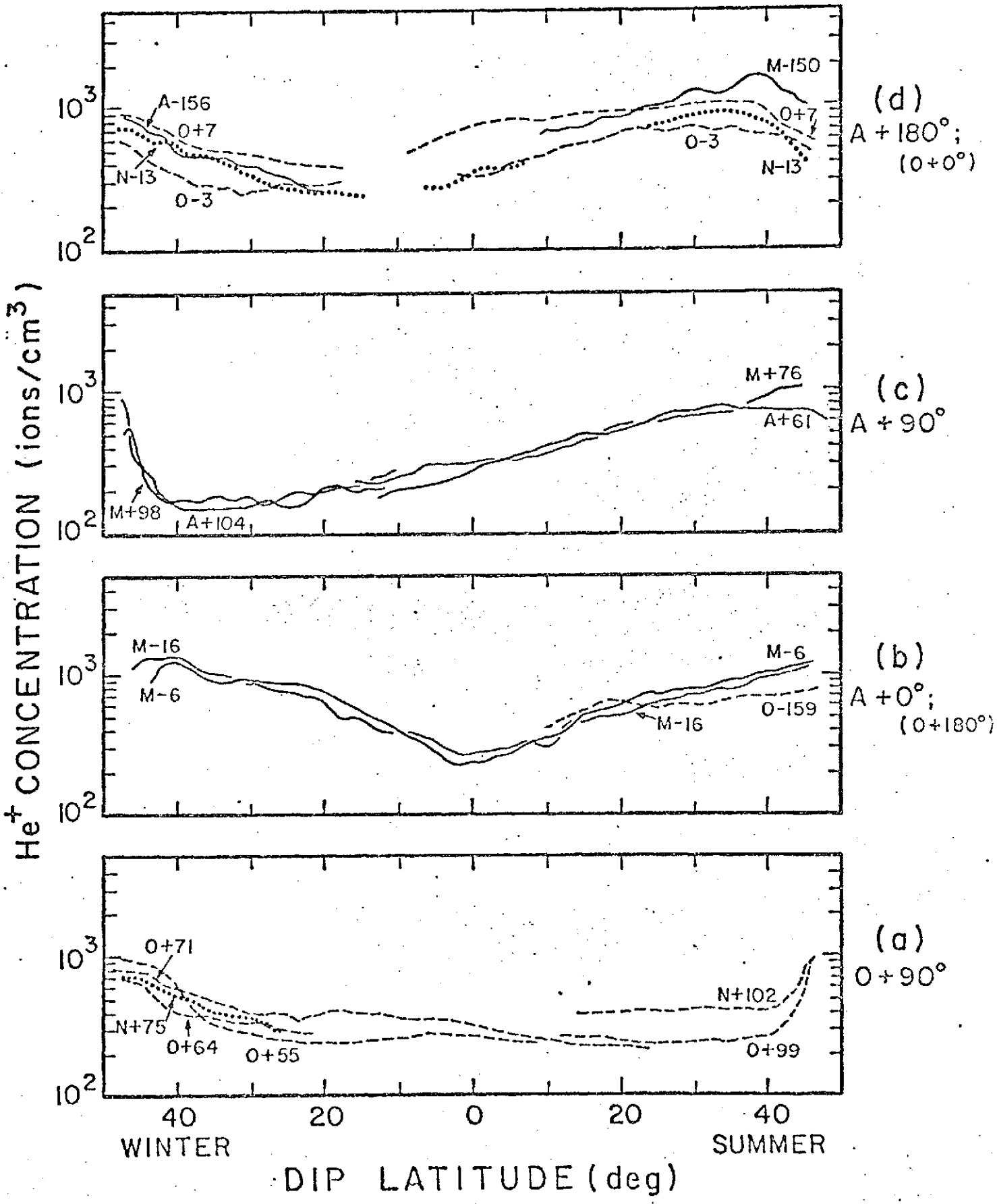
(d)
A + 180°;
(0+0°)
M-150
A-156
0+7
0+7
0-3
N-13
N-13
0-3
(c)
A + 90°
M+76
A+61
M+98
A+104
(b)
A +0°;
(0+180°)
M-16
M-6
M-6
0-159
M-16
(a)
0 + 90°
0+71
N+102
N+75
0+64
0+55
0+99
10^3
10^2
He^+ CONCENTRATION (ions/cm^3)
40
20
0
20
40
WINTER
SUMMER
DIP LATITUDE (deg)

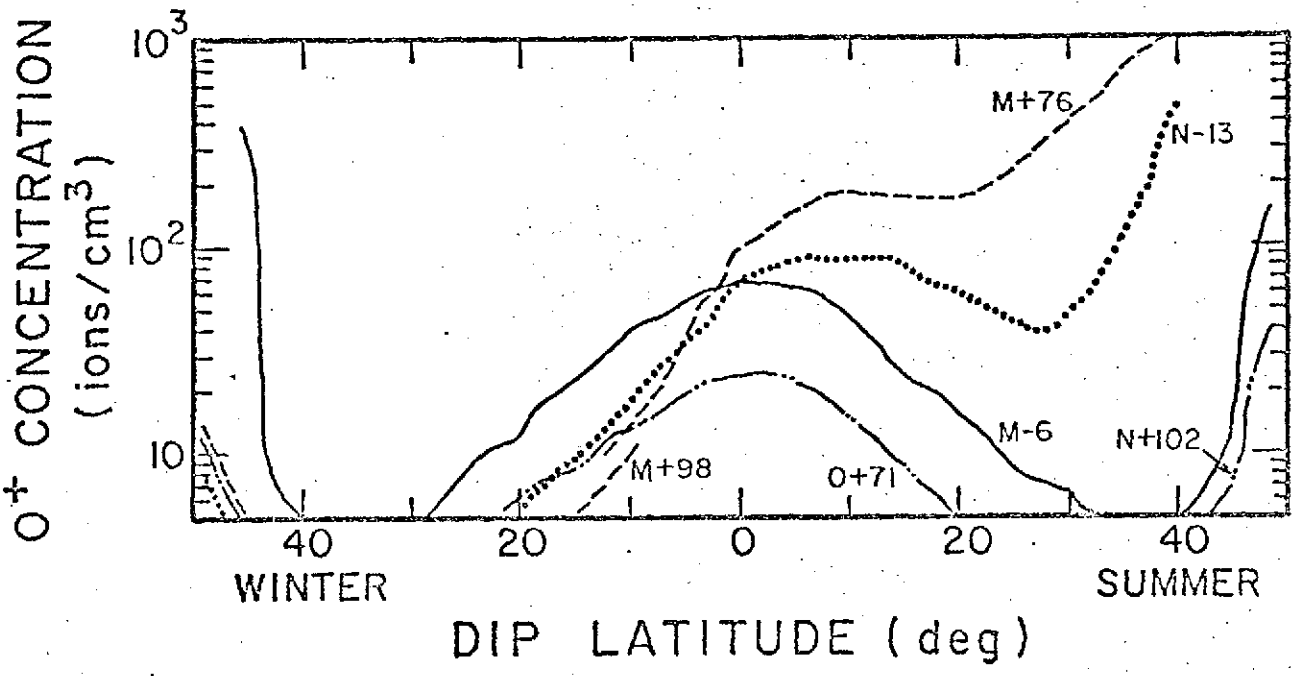
O+ CONCENTRATION (ions/cm3)
10^3
10^2
10
M+76
N-13
M-6
N+102
M+98
0+71
40
20
0
20
40
WINTER
SUMMER
DIP LATITUDE (deg)

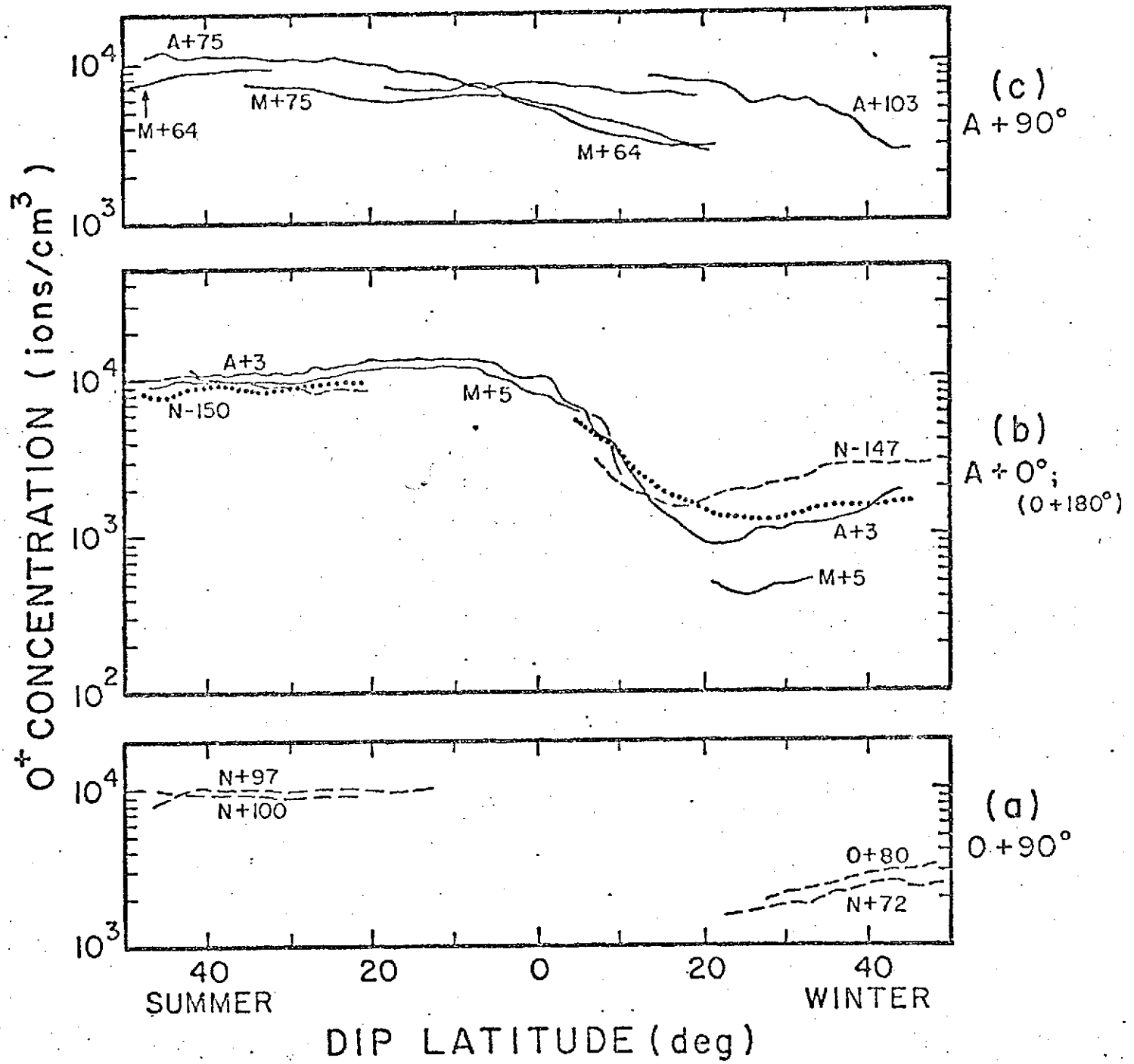
A+75
M+75
M+64
M+64
A+103
(c)
A + 90°
A+3
N-150
M+5
N-147
A+3
M+5
(b)
A ÷ 0°;
(0 + 180°)
N+97
N+100
0+80
N+72
(a)
0 + 90°
10^4
10^3
10^2
O^+ CONCENTRATION (ions/cm^3)
40
SUMMER
20
0
20
40
WINTER
DIP LATITUDE (deg)

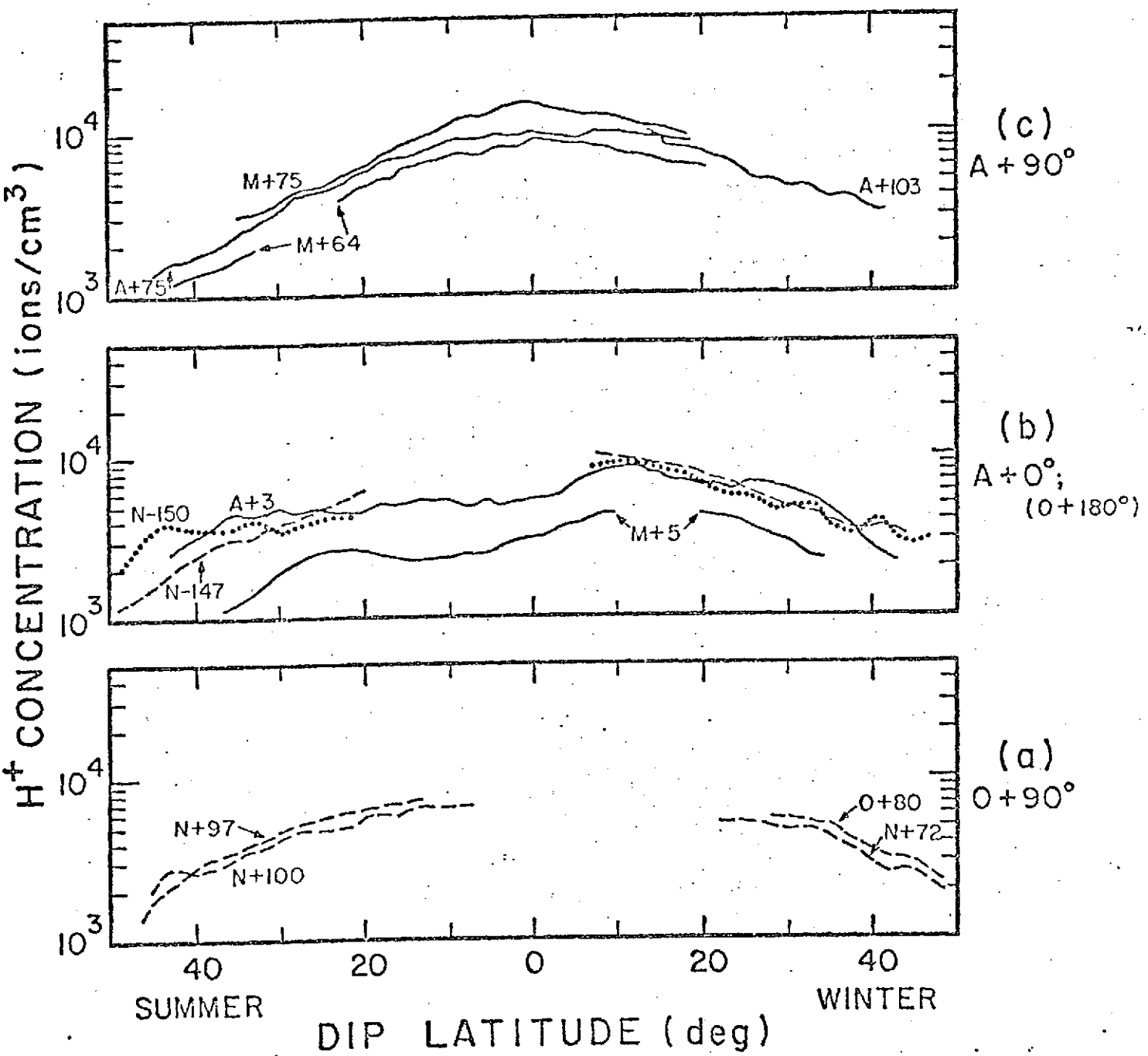
H+ CONCENTRATION (ions/cm3)
10^4
10^3
M+75
M+64
A+75
A+103
(c)
A + 90°
N-150
A+3
N-147
M+5
(b)
A + 0°;
(0 + 180°)
N+97
N+100
O+80
N+72
(a)
0 + 90°
40
20
0
20
40
SUMMER
WINTER
DIP LATITUDE (deg)

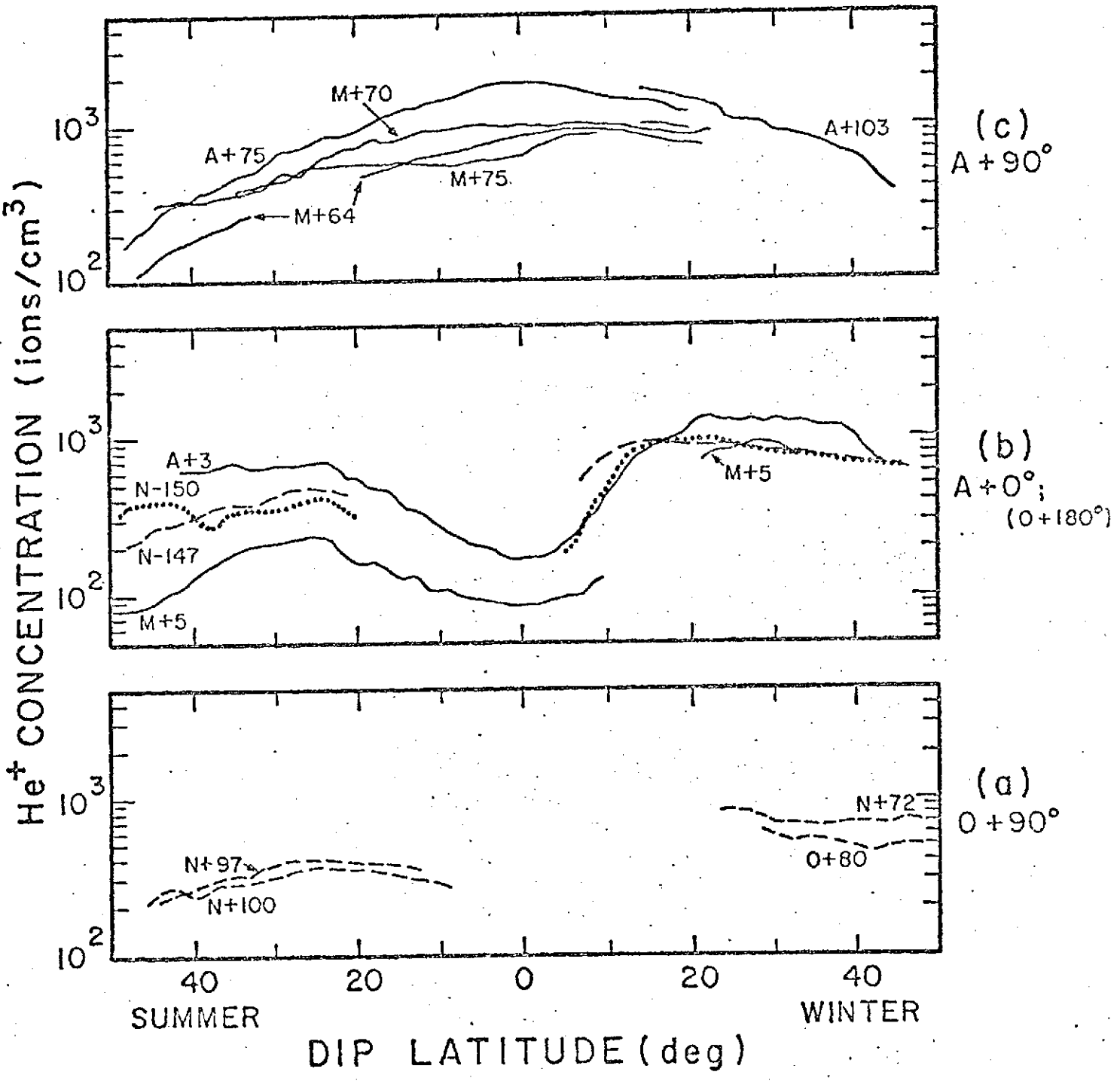
M+70
A+75
M+75
M+64
A+103
(c)
A+90°
A+3
N-150
N-147
M+5
M+5
(b)
A+0°;
(0+180°)
N+72
0+80
N+97
N+100
(a)
0+90°
He^+ CONCENTRATION (ions/cm^3)
10^3
10^2
40
20
0
20
40
SUMMER
WINTER
DIP LATITUDE (deg)

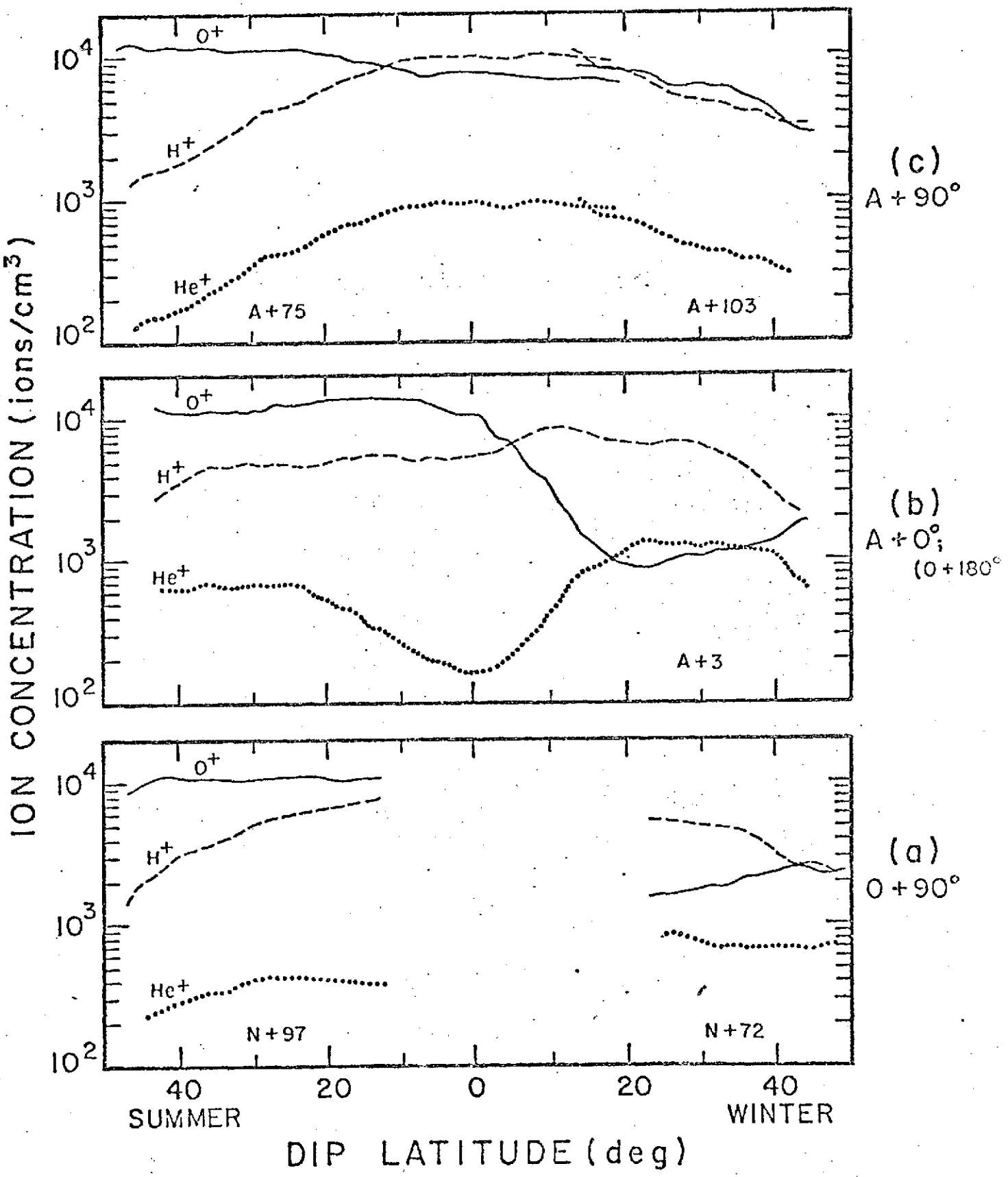
ION CONCENTRATION (ions/cm³)
10⁴
10³
10²
O+
H+
He+
A+75
A+103
(c)
A+90°
A+3
(b)
A+0°;
(0+180°
N+97
N+72
(a)
0+90°
40
20
0
20
40
SUMMER
WINTER
DIP LATITUDE (deg)

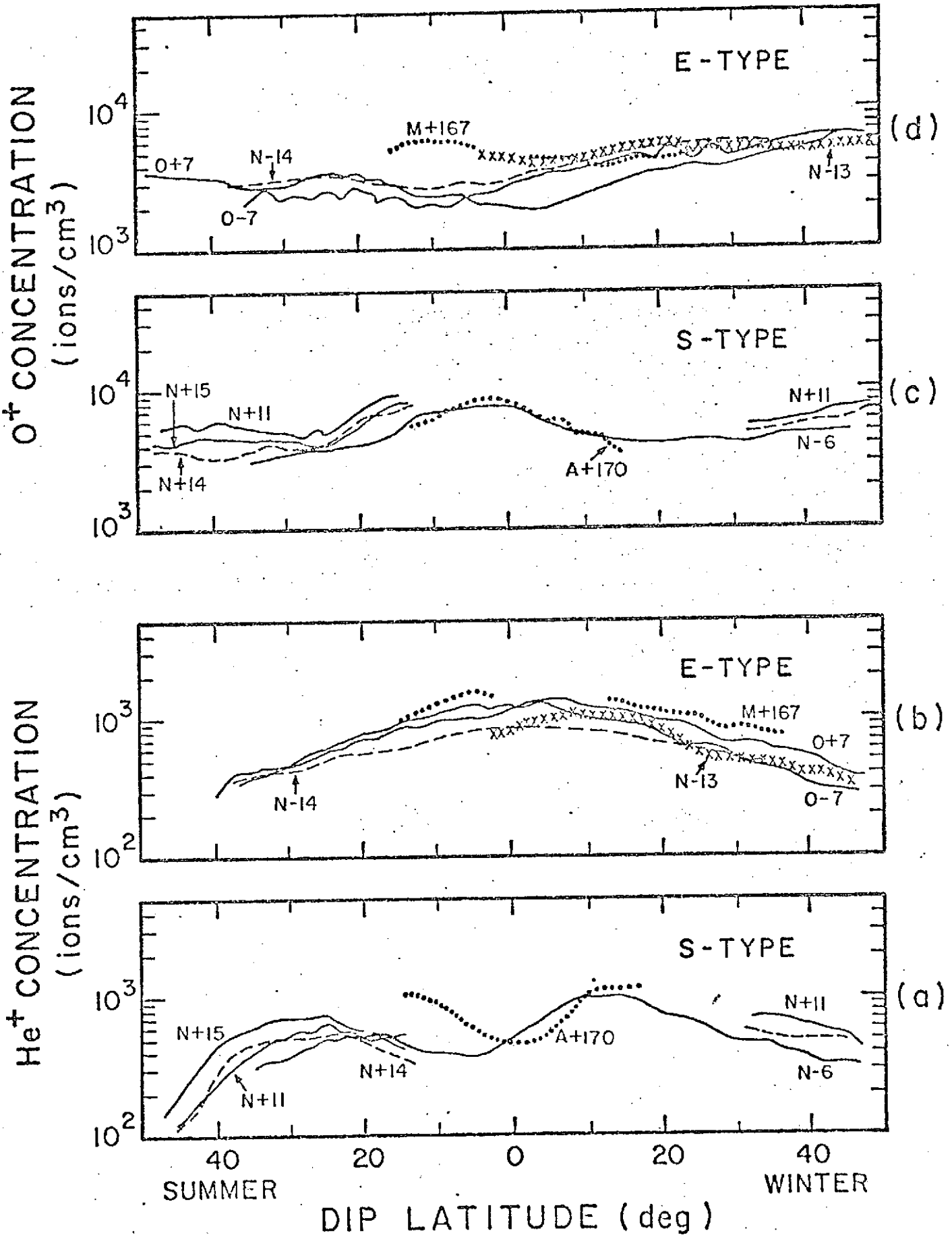
E-TYPE
M+167
O+7
N-14
O-7
N-13
(d)
S-TYPE
N+15
N+11
N+14
A+170
N+11
N-6
(c)
O+ CONCENTRATION (ions/cm3)
E-TYPE
M+167
O+7
N-13
N-14
O-7
(b)
S-TYPE
N+15
N+11
N+14
A+170
N+11
N-6
(a)
He+ CONCENTRATION (ions/cm3)
40
20
0
20
40
SUMMER
WINTER
DIP LATITUDE (deg)

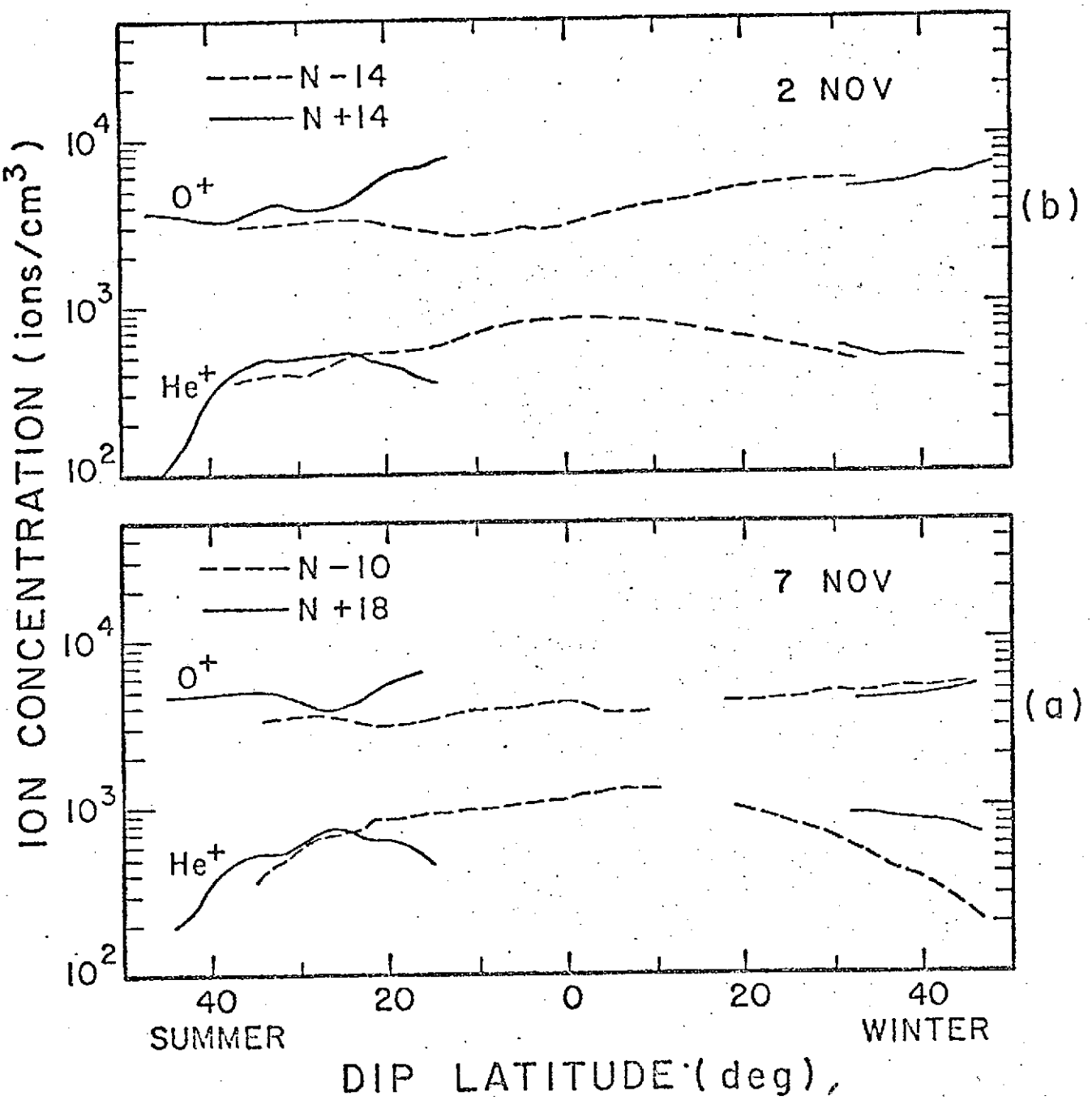
N-14
N+14
2 NOV
O+
He+
(b)
N-10
N+18
7 NOV
O+
He+
(a)
ION CONCENTRATION (ions/cm3)
10^4
10^3
10^2
40
20
0
20
40
SUMMER
WINTER
DIP LATITUDE (deg)

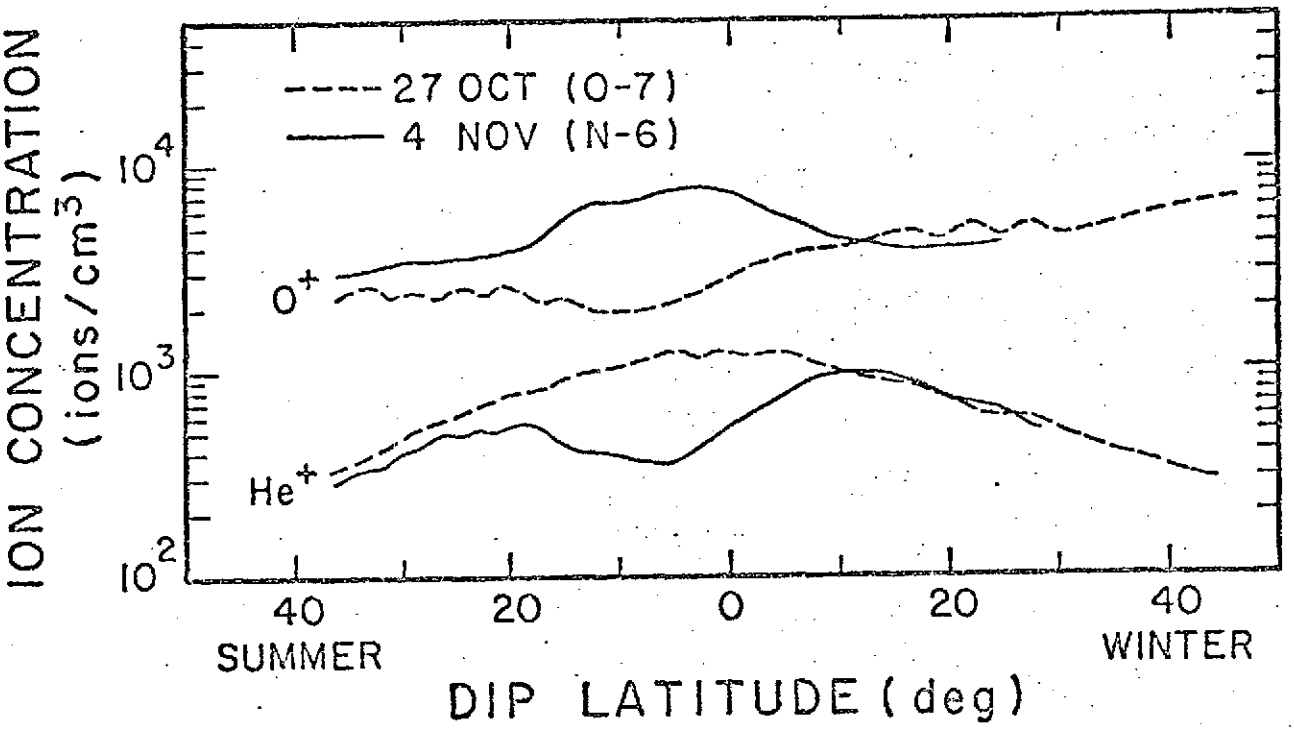
27 OCT (O-7)
4 NOV (N-6)
O+
He+
ION CONCENTRATION (ions/cm3)
10^4
10^3
10^2
40
20
0
20
40
SUMMER
WINTER
DIP LATITUDE (deg)

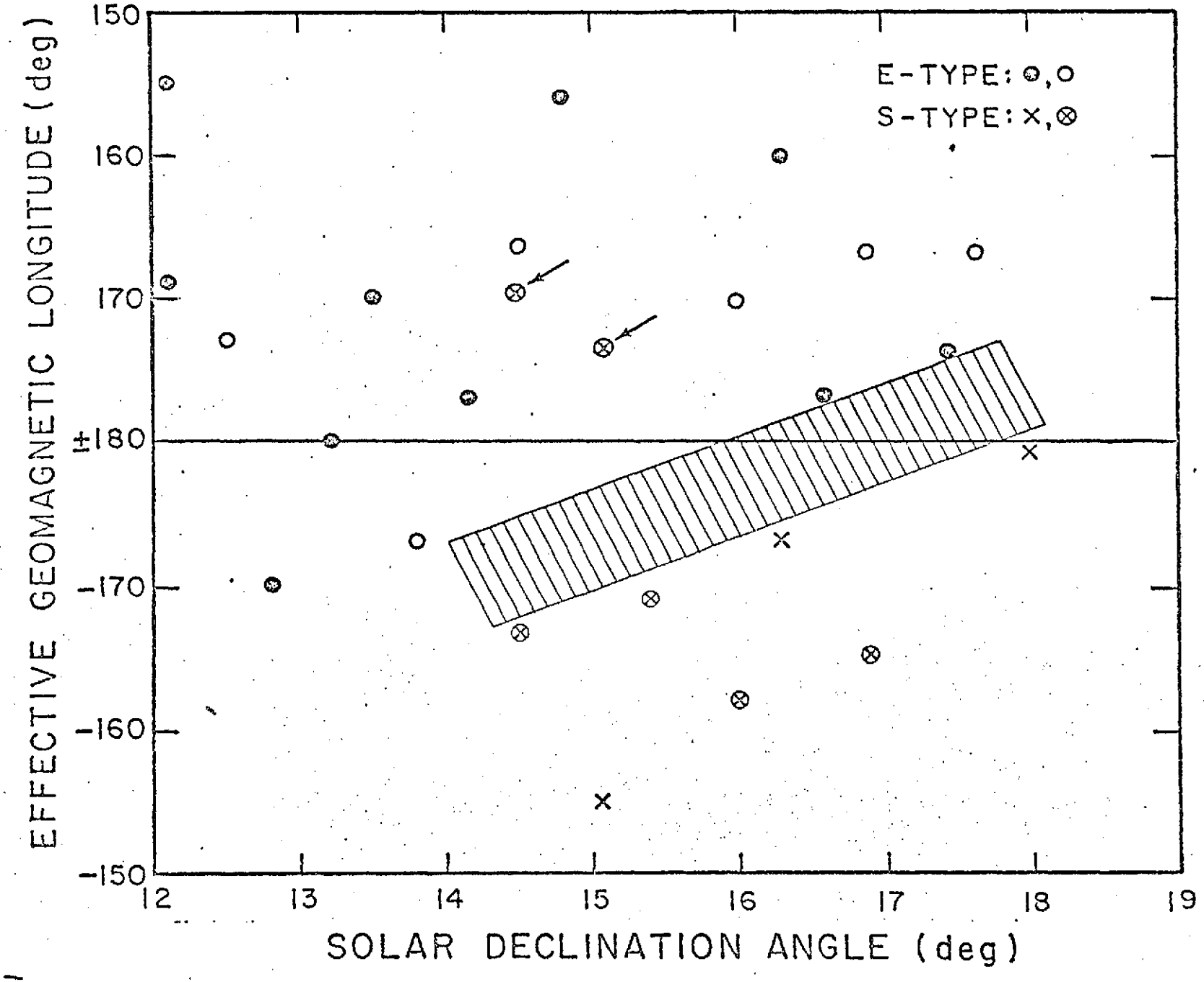
E-TYPE: ⊙,○
S-TYPE: ×,⊗
EFFECTIVE GEOMAGNETIC LONGITUDE (deg)
150
160
170
±180
-170
-160
-150
12
13
14
15
16
17
18
19
SOLAR DECLINATION ANGLE (deg)

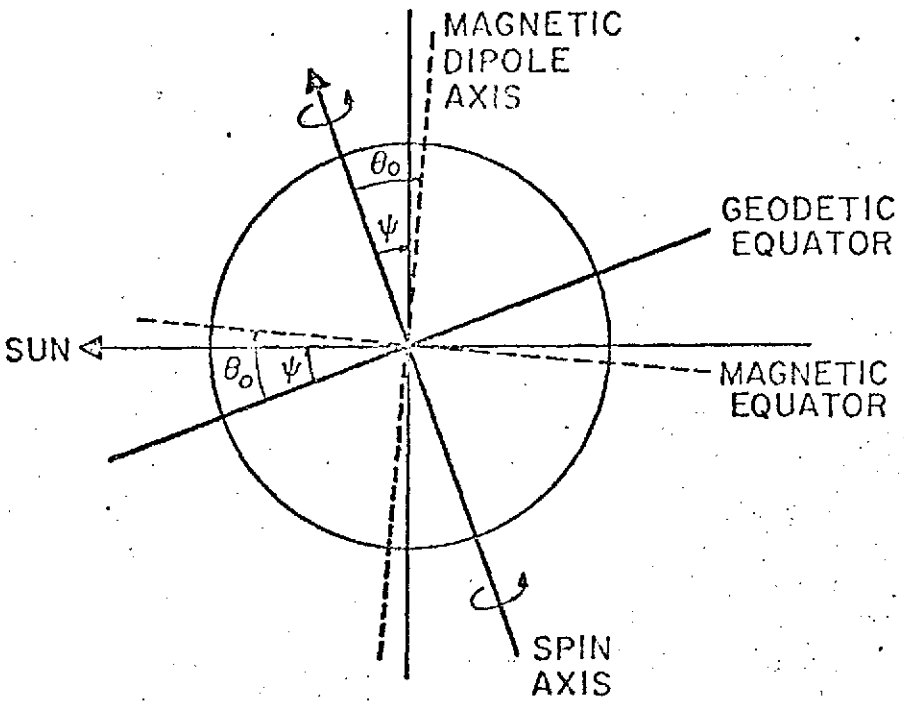

Initial Ion Composition Results From the Isis 2 Satellite

J. H. HOFFMAN, W. H. DODSON, C. R. LIPPINCOTT, AND H. D. HAMMACK

University of Texas at Dallas, Dallas, Texas 75230

Isis 2 satellite carried, among other ionospheric instruments, an ion mass spectrometer designed to measure the composition of the ionosphere in the mass range 1–64 amu. The satellite, in a nearly constant 1400-km orbit, was launched on April 1, 1971. Examples of data show a wide variation in ion composition from 99% H^+ at night near the equator to greater than 95% O^+ (and N^+) in the daytime poleward of the plasmapause. Both H^+ and He^+ are observed to be streaming outward from the high-latitude regions with velocities of several kilometers per second (the polar wind), determined from phase shifts in roll modulation maximums between light and heavy ion species. During the August 1972 magnetic storm a unique ionosphere developed consisting of N^+ as the dominant species between 55° and 80° invariant latitude (above the plasmapause) and N_2^+, NO^+, and O_2^+ at the 10^3-cm^{-3} concentration level, whereas these molecular species are usually below the detection limit of 1 ion cm^{-3} in quiet times at this altitude.

The Isis 2 satellite, launched on April 1, 1971, into an 88.1° prograde orbit with apogee and perigee of 1440 and 1360 km, respectively, carried a number of ionospheric sensors including an ion mass spectrometer. This instrument, a magnetic deflection mass spectrometer, was designed to identify and measure the concentration of the positive ions in the earth's upper atmosphere in the mass range 1–64 amu. Operation has been continuous with a 30% duty cycle for the past 3 years.

Large variations in ion composition are observed even at the constant altitude of 1400 km. Phase shifts between H^+ and O^+ roll modulation maximums, which indicate regions where polar wind particles are flowing, are a regular feature of both northern and southern high-latitude areas. Data taken during the large magnetic storm of August 1972 indicate large changes in ion composition, the molecular ion species playing an important role.

In this paper, discussion will center on a brief description of the instrument, in-flight calibration procedures, and preliminary data related to the scientific problems mentioned above. The paper is designed as an introduction to the rather large quantity of data accumulated from this instrument, which will be presented in more detail in forthcoming papers.

Instrument Description

The ion mass spectrometer consists of an entrance aperture, magnetic mass analyzer, and ion detection system as shown in Figure 1. The entrance aperture, a 7.6-cm-diameter screen mounted flush with the spacecraft surface, is oriented to look radially outward from the spacecraft. Ambient ions are attracted to the screen by a −6-V potential on the screen and by the usually negative satellite potential.

There are two basic orientation modes of the spacecraft, cartwheel and orbit-aligned. In the former the spin axis is normal to the orbit plane, this orientation allowing the spacecraft to roll (or skid) along the orbit such that the entrance aperture points alternately in the ram and wake directions. In the latter the spin axis lies in the orbital plane. The satellite velocity, which is large in comparison with ion thermal velocities (except for H^+), generates an ion flux toward the satellite in the reference frame in which the satellite is at rest. Since the portion of this flux that passes into the mass spectrometer is a strong function of angle of attack of the entrance aperture, the spinning motion of the spacecraft produces data that are roll-modulated, the modulation amplitude (ram to wake ion current ratio) being strongly mass dependent. Valid ion concentration data are obtained only when the angle of attack is near zero, the ram condition. The orbit-aligned case produces a favorable angle of attack only at 2 points along the orbit, the positions depending on the declination of the spin axis. For this reason, data presented herein have been taken only when the satellite is in cartwheel mode, in which the satellite was operated about 50% of the time.

Ions that pass through the entrance screen are accelerated through a narrow slit (the object slit), collimated into a beam, and passed through the magnetic analyzer. Two allowable ion trajectories, 1.8- and 5.1-cm radii, through the magnetic field lead to two collector slits positioned such that ions of mass ratio 1–8 can simultaneously reach the slits. The mass spectrum is scanned by varying the ion accelerating voltage, which has a repetitive exponentially decaying wave form with a 1-s period, over the range from 2000 to 250 V. This causes the mass ranges 1–8 and 8–64 amu to be swept simultaneously across the collector slits once each second.

Ions traversing each collector slit are detected by a magnetic strip electron multiplier (Bendix M310S), used as a current amplifier, and a logarithmic electrometer amplifier, one for each mass range. The dynamic range of each log amplifier is 2×10^{-12} to 1×10^{-6} A, producing an output voltage range from 0.2 to 5.0 V. Sensitivity of the instrument in flight is a few tenths of an ion per cubic centimeter, this very high sensitivity being due in part to the rapid motion of the satellite through the ionospheric medium.

The signals from each log amplifier are digitized to 8-bit words and fed into 'peak' circuits that detect the mass spectral peak amplitudes by a logic process involving peak location and amplitude averaging. The peak circuit is a unique feature of this instrument. It searches the output data from the log amplifiers for bona fide peaks (noise spikes are rejected) and determines the amplitude of each. Subsequently, these amplitudes are stored in buffer registers until they are sampled by the telemetry system. Since only the peak amplitudes are transmitted, a relatively small bandwidth suffices to read out the data. By using this technique the short sweep time of 1 s can be utilized effectively to produce 15–20 data points for each spectral peak for each satellite roll period (depending on spin rate). This data rate is sufficient to define the roll modulation curve for each ion species adequately. The position of

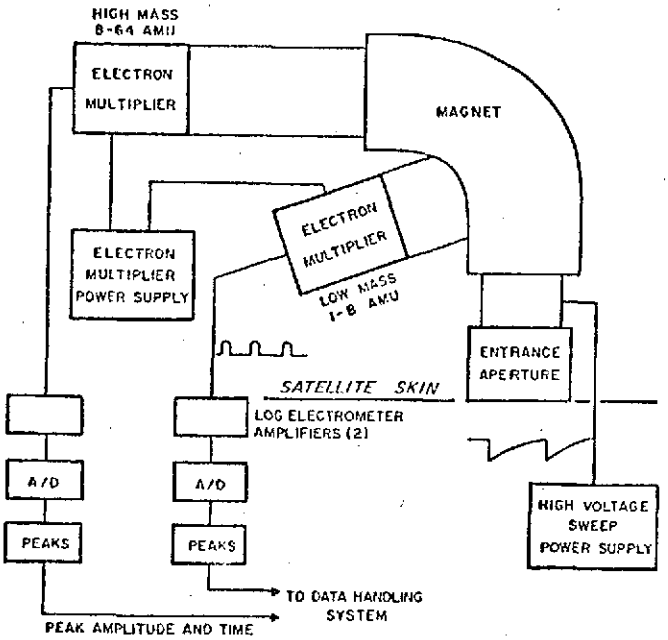

Fig. 1. Isis 2 ion mass spectrometer showing principal parts of instrument and major electronic assemblies. Use of two detector channels permits simultaneous scanning of two parts of mass spectrum, making it possible for the entire mass range from 1 to 64 amu to be swept in 1 s. The instrument is packaged in a rectangular box 15 × 12.5 × 33 cm, weighing 6.1 kg and mounted behind an equatorial panel of the spacecraft to look radially outward.

each ion peak in the telemetry format determines its mass number.

A backup diagnostic mode, called the analog mode, is available in which the spectral scan time is increased to 8 s, the peak circuits are disabled, and the entire mass spectrum is telemetered. This mode is used once each week for 2 min to monitor instrument operation via a quick look data handling process.

Instrument Calibration

An ion mass spectrometer measures relative abundances of the ions sampled from the ionosphere but can be calibrated to give absolute ion concentrations. Several factors cause the spectrometer to discriminate against ions of heavy mass. First, the instrument scans the mass spectrum by varying the ion accelerating voltage in an exponential manner from 2000 to 250 V. Lower mass ions are measured near the high voltage end of the sweep where the instrument has a higher transmission factor than at the low voltage, high mass end. This phenomenon is known as the voltage effect. Second, light mass ions, being more mobile than heavy mass ions, are collected from a larger volume. Hence a larger light mass ion current is measured for equal concentrations of light and heavy mass ions.

The only practical method of calibration of an ion mass spectrometer is an in-flight procedure [*Hoffman*, 1969; *Hoffman et al.*, 1973] in which the sampling efficiency of the various ion species from the plasma was done by comparing the total ion current (the sum of all the peaks) with electron density data from the ionograms produced from the sounder experiment on board Isis 2 (J. Whitteker, private communication, 1973). Comparisons were first made in regions where the ionosphere consisted of greater than 95% H^+ ions (the remainder being mainly He^+ and D^+). Thus a direct calibration of the absolute sensitivity of the mass spectrometer to H^+ was obtained. Next, a similar calibration was made for O^+ by using ionospheric regions that were greater than 90% O^+. In this case the calibration for H^+ was incorporated into the calculation. The He^+ calibration had been inferred from the above, but recently, a region of He^+ dominance was identified and a direct He^+ calibration obtained. From the 3 point calibration the sensitivity factors for the minor ions were obtained.

A typical example of the result of this in-flight calibration procedure is shown in Figure 2. In pass 339 the ion composition changes from predominantly O^+ to H^+ at −5° and back to O^+ at −45° latitude. In pass 345 the composition changes from predominantly H^+ below to O^+ above 55° latitude. Figure 6 shows the detailed composition of this pass. Agreement between the total ion concentration N_i, as determined by the sum of the individual ion species concentrations, and the electron density is generally better than 20% regardless of which ion is the dominant species except perhaps in highly structured regions.

The mass spectrometer measures the ionospheric parameters in the immediate vicinity of the spacecraft. That is, it can only detect those ions that arrive at the instrument entrance aperture, whereas the sounder electron density measurement is an integral result of the electron density near the spacecraft. In highly structured regions these two may not always track. In addition, the calibration coefficients (sensitivity factors), which are determined by this comparison process, are thought to be somewhat dependent on total ion density and composition, ion temperature, and spacecraft potential [*Parker and Whipple*, 1970; *Whipple et al.*, 1974]. Nevertheless, these effects seem to be sufficiently small to enable the mass spectrometer to produce ion concentration measurements to better than 20% accuracy as compared with simultaneous electron concentration data, such as those obtained from the top side sounder.

Results

Ion composition data are available in two basic formats, both reproduced on microfilm. Ion peak amplitudes, identified by mass number and converted to concentrations, are plotted as a function of time, ephemeris data being listed along the abscissa. Figure 3 is an example of such a plot showing only O^+, He^+, and H^+ for clarity. All the ion species normally appear on this type of plot. The data clearly show the roll modulation effect of a spinning satellite. If all the ion species have merely thermal velocities, the roll modulation maximums will be coincident in time and coincide with the ram direction (zero angle of attack). See cosine curve in Figure 3. However, if one ion species velocity contains a bulk motion term, its maximum will be shifted away from ram in the direction of the resultant between the satellite velocity and bulk velocity vectors. By observing the magnitude of this phase shift and knowing the satellite velocity, the bulk velocity can be calculated. Polar wind velocities are easily measured by this process. In the example of Figure 3 the H^+ velocity is 4.2 km s^{-1}, and the H^+ flux is 1.3×10^8 ions cm^{-2} s^{-1}.

The He^+ also frequently exhibits a phase shift with respect to O^+ and the ram direction with a magnitude usually about one half that of H^+. In the present example the He^+ velocity and flux are 2 km s^{-1} and 9×10^6 ions cm^{-2} s^{-1}, respectively.

The H^+ wake enhancement is a commonly observed phenomenon, but its origin has not been studied in detail. A

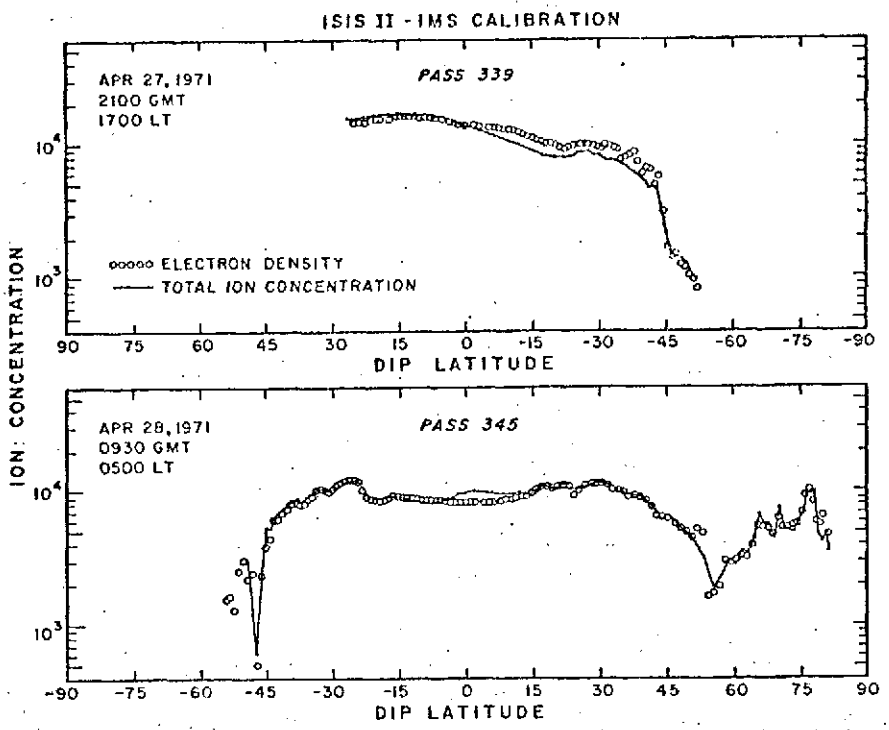

Fig. 2. In-flight calibration result showing comparison of total ion composition and electron density from on-board top side sounder. Agreement is generally better than 10%. In pass 339 the ion composition is predominantly H^+ between −5° and −45° latitude and O^+ both farther northward and southward. Composition changes from dominantly H^+ below to O^+ above 55° latitude in pass 345.

number of satellite wake studies have been conducted, but these are mainly theoretical, and very little comparison between theory and experiment has been done [*Samir and Jew*, 1972]. From the data exhibited here, it appears that the light ions are capable of reaching the instrument when it is pointing in the wake, as has been shown by *Samir et al.* [1973], and in certain preferred directions (not exactly in the wake) there appears to be a channel through which ions are more readily transported to the instrument.

Roll modulation maximums plotted as a function of dip latitude, other ephemeris data being listed along the abscissa, produce a pole-to-pole plot, such as Figure 4. This is primarily a daytime (late afternoon) ionosphere showing both winter in the southern hemisphere and summer in the northern hemisphere at the essentially constant satellite altitude of 1400 km. The constancy of the Isis 2 orbit is a great advantage in presenting such data because latitudinal and local time variations can be studied without the usual complications introduced by simultaneous altitude changes. In this case the satellite is in sunlight, but at −45° dip latitude the satellite crosses the terminator passing into a region where a part of the ionosphere below the spacecraft is in darkness. The O^+ is the dominant species in the summer day above +20° dip latitude, and its concentration remains very flat all the way to the pole, showing no evidence of a high-latitude trough. The H^+, although it is dominant at the equator, decreases gradually until 45°N, where a steep negative gradient, indicative of the plasmapause, is observed. It then remains fairly flat out to the pole at a level a factor of 30–40 below the O^+. The He^+ tends to follow H^+ at about 1 order of magnitude lower, showing the plasmapause gradient and equatorial bulge. The behavior of O^+ and He^+ in the equatorial to mid-latitude region is longitude dependent, as is discussed by *Breig and Hoffman* [1974]. In Figure 4 the absence of an equatorial trough is typical of the +90° longitude case discussed in the reference.

In the southern hemisphere, H^+ is the dominant ion from the equatorial maximum to −40°, where O^+ exhibits a small enhancement centered about −42°. The He^+ tends to follow H^+ until −30°, where its rate of decrease is less, with the result that He^+ becomes the dominant ion species between −50° and −58°, albeit, at a concentration of less than 300 cm^{-3}. (The He^+ region is not always present.) The sharp trough at −50° in all ion species is coincident with an upward flow of H^+ of 2 km s^{-1} (polar wind), although the flux at this point is very low owing to the low H^+ concentration. Farther poleward, O^+ again becomes the dominant species.

The details of the winter polar region are shown in Figure 5. The left-hand side of the plot is an extension of Figure 4 showing the O^+ peak at −42°, the region of He^+ dominance, and the O^+ peak at −66°. This peak is a consequence of the polar

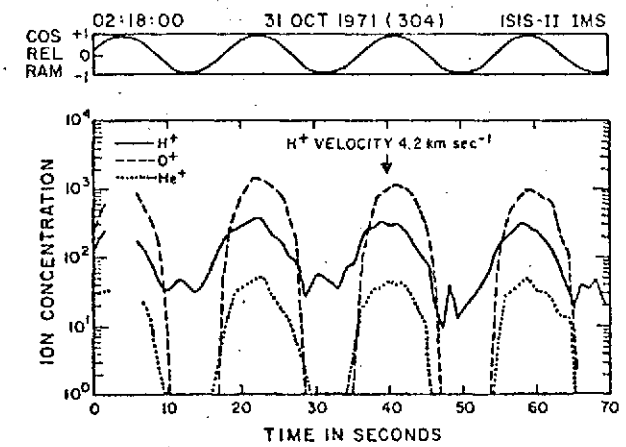

Fig. 3. Roll modulation curve showing ion concentrations as a function of time with ephemeris data along abscissa. When cosine of relative ram angle is 1.0, angle of attack is zero. Phase shift between O^+ and H^+ roll modulation maximums is a measure of the polar wind velocity.

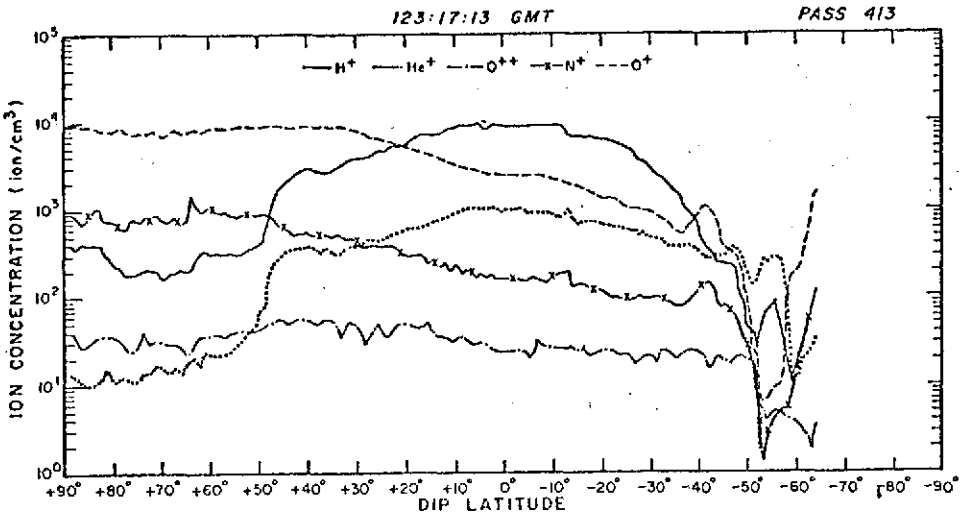

Fig. 4. Pole-to-pole plot of ion daytime concentrations. Northern summer is to the left and southern winter to the right. Local time is 1713–1810. Satellite altitude is essentially constant at 1400 km. At about −45° latitude the solar zenith angle exceeds 90°, but the orbit altitude is still sunlit.

wind, which establishes a parallel electric field along open magnetic field lines that increases the scale height of the ionosphere. The light ions have largely been depleted by the flow, and thus O^+ is being left as the dominant species. The winter polar cap region is generally characterized by a very low ionic concentration, as it is in darkness, and no source of photoionization is present there. Toward the night side the pattern is essentially repeated except that the O^+ concentration becomes very low toward mid-latitude owing to the lower nighttime ion temperature.

Figure 6, a nighttime (0500) pole-to-pole pass a few days earlier than the passes in Figures 4 and 5, shows H^+ to be the dominant constituent between ±45°. A steep gradient in H^+, indicative of the plasmapause, occurs at ±50°, followed by a trough with O^+ dominance poleward that is fairly flat in the summer but has considerable structure in the winter (Figure 5). These are again the regions of polar wind flow. Concentrations of H^+ are down by a factor of 100 above the

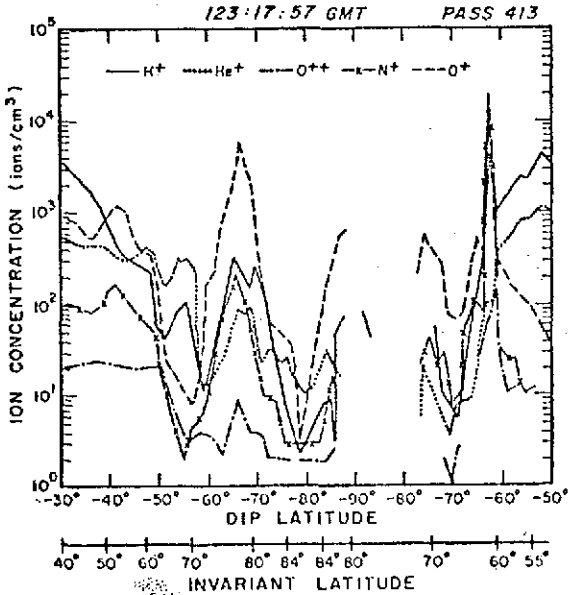

Fig. 5. Polar region of winter ionosphere at 1400 km. To the left is daytime, an extension of Figure 4 (0400 LT), and to the right is nighttime (0400 LT). Large O^+ peak at −62° (night) identifies region of polar wind activity.

plasmapauses. The He^+ exhibits a marked dip at the equator, with mid-latitude peaks just equatorward of the plasmapause and a very steep gradient at the plasmapause. Farther poleward, the concentration is less than 10 ions cm^{-3}. However, the He^+ behavior is quite longitude dependent [*Breig and Hoffman*, 1974], the equatorial dip being especially pronounced near 0°, the longitude of the data in Figure 6. The O^+ appears to be anticorrelated with He^+ at the equator and mid-latitudes and exhibits a steep positive gradient at the light ion plasmapause before becoming the dominant species toward the poles. The polar cavity that exists in the winter appears to be filled with principally O^+ ions in summer.

Taylor [1972] and *Chandra* [1974] have shown data from Ogo 4 and 6 ion mass spectrometers that confirm the He^+ and O^+ nighttime distributions shown here. Chandra relates the behavior of these distributions to the geomagnetic anomaly, the electrodynamic lifting of ionization in the equatorial region, and its subsequent diffusion along the field lines. As the spacecraft cuts across field lines, the observed ion concentration distribution reflects the vertical profile of each constituent at the equator.

Generally, O^{++} follows O^+ at a concentration level 100–200 times lower in summer daytime but approaches the O^+ value in the winter trough. In the nighttime mid-latitude regions where O^+ is less than 10 ions cm^{-3}, O^{++} lies within a factor of 3 of O^+, especially in the summer. At higher latitudes where O^+ becomes dominant, the nighttime ratio returns to the order of 100.

The N^+ ions seem to track O^+ rather consistently at roughly 1 order of magnitude lower concentration except at mid- to low-latitude daytime (Figure 4), where the O^+/N^+ ratio is more like 20, and at night (Figure 6), where on each side of the equatorial O^+ maximum the ratio is as low as 3. However, at these exceptional times the N^+ concentration is of the order of 5 ions cm^{-3}, making the uncertainty in the measurements greater but still probably less than 50%.

The tracking of N^+ with O^+ is typical of all quiet time ionospheres. However, during the greatly disturbed time of the August 1972 magnetic storm at about 1700 LT, August 4, N^+ becomes the dominant ion, exceeding O^+, from 55° invariant latitude toward the pole, as is shown in Figure 7. During this time the 3-hour *Kp* index was 9. At the same time the three

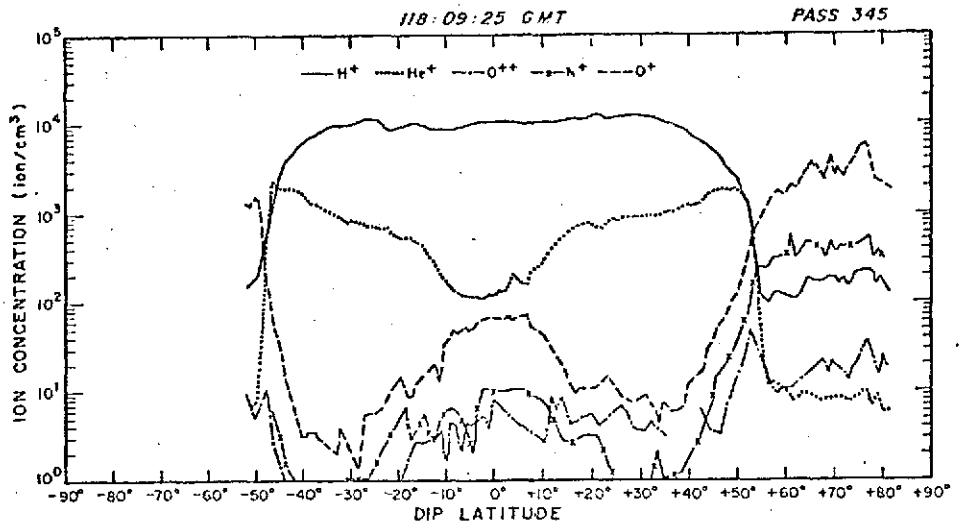

Fig. 6. Nighttime pole-to-pole plot of ion composition at 1400 km and 0500 LT. Summer is to the right and winter to the left.

molecular ion species, N_2^+, NO^+, and O_2^+, are observed for the first time at 1400 km. Under normal conditions they are below the detection limit, 1 ion cm^{-3}, of the instrument. Concentrations in the 10^3-cm^{-3} range are therefore highly unusual, as is the N_2^+ dominance over the other molecular species. In the normal E and F regions, N_2^+ is a very minor species compared with NO^+ and O_2^+ because N_2^+ ions, although they are formed by photoionization in the 150- to 200-km range, rapidly charge exchange with O and O_2 forming NO^+ and O_2^+.

Data from the Esro 4 mass spectrometer [*Prölss and von Zahn*, 1974] have shown a marked decrease in the neutral O/N_2 ratio and a corresponding enhancement of neutral N_2 at relatively high altitudes during the large magnetic storm (Kp = 7+) of February 21, 1973. (No neutral composition data are available for the August 1972 storm.) The excess high-altitude N_2 is ionized, but because neutral gas concentrations (O and O_2) above 300 km are much less than in the 150- to 200-km range, the charge exchange reactions cannot proceed as rapidly, and thus much of the ionization is being left in the form N_2^+. The high molecular ion concentrations are further supported by the high ion temperature, approximately 4000 K, measured during this phase of the storm (E. Maier, private communication, 1973). *Taylor* [1973] observed from the Ogo 6 satellite a large enhancement of NO^+ during the storm of March 8, 1970, at an altitude of 400–600 km (it is not clear from the reference that N_2^+ and O_2^+ are also enhanced at this time). In that case, O^+ remained the dominant species instead of N^+, possibly because Taylor's measurements were at a lower altitude or because the magnitude of the 1970 storm may have been less than that of the 1972 storm. Simultaneous measurements from the Ogo 6 neutral mass spectrometer showed an N_2 enhancement confirming the Esro 4 results.

Essentially all of the region at 1400 km where molecular ions are important lies above the plasmapause, located by a steep negative gradient in H^+, which in this case occurred at 55° invariant latitude (L = 3). *Brace et al.* [1974] have shown that during various phases of the development of the storm the plasmapause was depressed as far south as L = 1.9. The H^+ concentration remains rather low ($<10^2$ cm^{-3}) throughout the polar region but begins an upward trend toward the night side of the polar cap, where the molecular species are rapidly disappearing.

Conclusion

The ion mass spectrometer on the Isis 2 spacecraft identifies and measures the concentration of the positive ion constituents of the ionosphere. Examples of the data show a wide variation in the composition of the ionosphere at the nearly constant altitude of 1400 km from 99% H^+ at night near the equator to greater than 95% O^+ (and N^+) in the daytime poleward of the plasmapause. One of the advantages of the Isis 2 orbit is that owing to its constant altitude, latitudinal and local time variations may be investigated without the usual complexity introduced by corresponding altitude changes. The summer polar region (postplasmapause) is generally filled with O^+, both day and night, whereas the winter pole exhibits a deep cavity nearly void of ionization with sharp enhancements of O^+ just poleward of the plasmapause. Phase shift measurements between the roll modulation maximums of the light and heavy ion species provide particle velocities that are applicable to studies of the polar wind phenomenon, which is the subject of a forthcoming paper [cf. *Hoffman*, 1974].

The large magnetic storm in August 1972 produced a unique ionosphere at 1400 km, N^+ being the dominant species and N_2^+, NO^+, and O_2^+ having concentrations in the 10^3-cm^{-3} range. The region of interest lies poleward of the plasmapause,

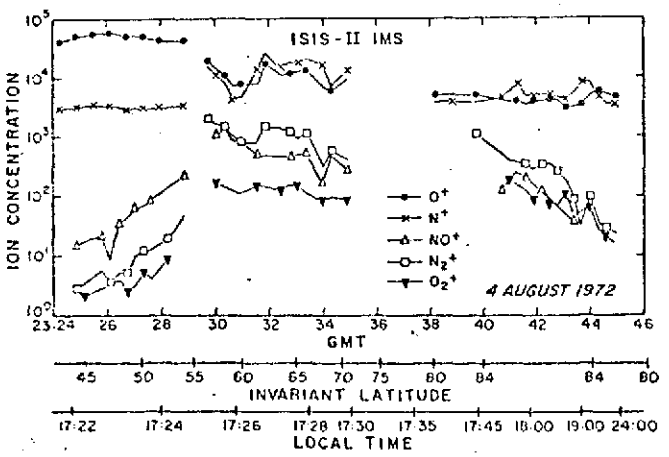

Fig. 7. Ion composition during August 1972 magnetic storm. Note N^+ dominance and high concentrations of molecular ion species. Because the plasmapause is highly depressed in latitude (L = 3.0), the molecular ion region lies in the transplasmapause region.

which is highly depressed in latitude during the storm. Neutral mass spectrometer data during a similar storm period in February 1973 show an N_2 enhancement at relatively high altitude, which could be the source of the N^+ and N_2^+.

Acknowledgements. The authors are indebted to Don R. Zuccaro, Larry D. Brooks, Loyd A. Swaim, Chester Shippy, and Ben J. Holt for the design and development of the instrument. The work was supported by the National Aeronautics and Space Administration contract NAS5-11003.

* * *

The Editor thanks R. S. Narcisi and C. Y. Johnson for their assistance in evaluating this paper.

REFERENCES

Bracc, L. H., E. J. Maier, J. H. Hoffman, J. Whitteker, and G. G. Shephard, Deformation of night side plasmasphere and ionosphere during August 1972 geomagnetic storm, submitted to *J. Geophys. Res.*, 1974.

Breig, E. L., and J. H. Hoffman, The mid- and low-latitude ionosphere at 1400 km from Isis 2 satellite, submitted to *J. Geophys. Res.*, 1974.

Chandra, S., The equatorial helium ion trough and the geomagnetic anomaly, *J. Atmos. Terr. Phys.*, in press, 1974.

Hoffman, J. H., Ion mass spectrometer on Explorer 31 satellite, *Proc. IEEE*, *57*(6), 1063, 1969.

Hoffman, J. H., The polar wind (abstract), *Eos Trans. AGU*, *55*, 69, 1974.

Hoffman, J. H., W. B. Hanson, C. R. Lippincott, and E. E. Ferguson, The magnetic ion-mass spectrometer on atmospheric Explorer, *Radio Sci.*, *4*, 315, 1973.

Parker, L. W., and E. C. Whipple, Jr., Theory of spacecraft sheath structure, potential, and velocity effects on ion measurements by traps and mass spectrometers, *J. Geophys. Res.*, *75*, 4720, 1970.

Prölss, G. W., and U. von Zahn, Esro 4 gas analyzer results, 2, Direct measurements of changes in the neutral composition during an ionospheric storm, *J. Geophys. Res.*, *79*, 2535, 1974.

Samir, U., and H. Jew, Comparison of theory with experiment for electron density distribution in the near wake of an ionospheric satellite, *J. Geophys. Res.*, *77*, 6819, 1972.

Samir, U., E. J. Maier, and B. E. Troy, Jr., The angular distribution of ion flux around an ionospheric satellite, *J. Atmos. Terr. Phys.*, *35*, 513, 1973.

Taylor, H. A., Jr., Observed solar geomagnetic control of the ionosphere: Implications for reference ionospheres, *Space Res.*, *12*, 1275, 1972.

Taylor, H. A., Jr., Storm time relationships observed between H^+ and NO^+, Some implications for chemistry and dynamics (abstract), *Eos Trans. AGU*, *54*, 386, 1973.

Whipple, E. C., J. M. Warnock, and R. H. Winkler, Effect of satellite potential on direct ion density measurements through the plasmapause, *J. Geophys. Res.*, *79*, 179, 1974.

(Received February 19, 1974;
accepted June 20, 1974.)

79, NO. 16 JOURNAL OF GEOPHYSICAL RESEARCH JUNE 1, 1974

Observation of a Two-Temperature Ion Energy Distribution in Regions of Polar Wind Flow

E. J. MAIER

Goddard Space Flight Center, Greenbelt, Maryland 20771

J. H. HOFFMAN

University of Texas at Dallas, Dallas, Texas 75230

In many regions of the ionosphere the distribution functions of the particles are highly time dependent because of the variation in energy deposition and particle ionization rates. At present, it is recognized that the electrons, the ions, and the neutral gases exist at three generally distinct temperatures that approach one another at low altitudes, where the mutual collision frequencies are sufficiently high. In the high-latitude region, and especially at higher altitudes, a greater deviation from equilibrium is expected as a consequence of the complex flow patterns of ionization, downward energy conduction, and mass flow. In this work we begin a study of deviations from thermal equilibrium among the ions by considering that the 'light' ions H^+ and He^+ may be at a different temperature from the 'heavy' ion O^+. Further, we study in particular the case in which thermal protons are observed to be flowing relative to the assumed static ambient oxygen ions. The proton flow is assumed to be along the direction of the magnetic field. Of the cases tested, it is found that the measured proton temperature is from 1 to 10 times the measured oxygen ion temperature. Such temperature enhancements may be expected both because of the energy transfer associated with the ion flow and as a consequence of the preferential energy coupling from the light ion distribution in the exosphere.

The general problem of defining in detail the distribution functions of the many species of particles present in the ionosphere is exceedingly complex. In the low-altitude region, where collision frequencies are sufficiently high, the kinetic contact between the various species insures that a state of thermal equilibrium obtains. As particle density decreases with altitude, however, the situation becomes more complex. In addition to simple kinetic elastic collisions the various species enter into particular reactions and energy exchange processes with the particles and fields that are present. Such a situation is essentially nonequilibrium in nature as a result of the variety of the final states of particles after their chemical or field interaction. A further condition contributing to the nonequilibrium nature of the situation is that the system is time dependent on a scale comparable to, or more rapid than, the time for complete relaxation to a final state.

A variety of factors contribute to the time variation of the system. The solar and particle ionizations, which are the basic production mechanisms for the ionic species, are highly time dependent, especially at high latitudes, where energy deposition can be extremely localized. The coupling between the ionosphere and the plasmasphere-magnetosphere system is both time and geomagnetic activity dependent. Finally, there are energy exchanges associated with dynamic processes: Examples of these are neutral wind ion drag, polar wind ion flow, and ion plasma expansion. Ultimately, it is the ratio between the thermalization time (the collision time between identical or noninteracting particles) and the 'excitation' time (the time between interactions with other particles or the time to exchange energy to a local field) that determines the degree of relaxation toward thermal equilibrium. It has generally been considered that the particle distributions in the ionosphere can be described by three temperatures: T_e, the electron temperature; T_i, the ion temperature; and T_n, the neutral gas temperature. In this paper we report initial observations of deviation from simple Maxwell-Boltzmann equilibrium of the thermal ions in regions of the ionosphere having a polar wind flow of light ions (hydrogen and helium) through an assumed static distribution of oxygen ions.

Experimental Considerations

Two experiments on the Isis 2 spacecraft were used to define the velocity distribution of the ions. The planar retarding potential analyzer (RPA) was used to measure the component of ion flux into the instrument in the 0- to 10-eV energy range. The ion mass spectrometer (IMS) data were used to define the existence of a flow of the light ions with respect to the heavy ions and thus to determine the mean velocity of the light ions. Here the scan over velocity direction was made by the rotation of the spacecraft about its spin axis.

The experiment configuration is illustrated in Figure 1. In one mode of operation, the 'cartwheel' mode, the spacecraft spin axis is perpendicular to the spacecraft orbital plane. Thus all experiments mounted on the spacecraft equatorial plane sample particle fluxes from all directions in the spacecraft orbital plane once per spacecraft rotation. These ion fluxes have as one velocity component the 'ram' flow proportional to the 7-km/s spacecraft velocity. As is indicated in the figure, the instruments view first along the spacecraft velocity vector and then, a fraction of a spacecraft rotation later, along the direction of the earth's magnetic field facing downward. If there exists a bulk flow of one species of ion up the magnetic field, the relative direction with respect to the spacecraft will be as indicated in the insert to Figure 1. A typical 'spin' modulation curve obtained from the IMS in a region with an observed difference between the apparent light ion flow and the heavy ion flow is shown in Figure 2. In this example, the instrument observed a maximum proton flux about 2 s before it observed a maximum O^+ flux. For the 18-s spacecraft spin period this observation implies an apparent difference in direction of 40°. It is assumed that the apparent O^+ flow is only the ram flow resulting from the spacecraft motion. The H^+ flow is taken to

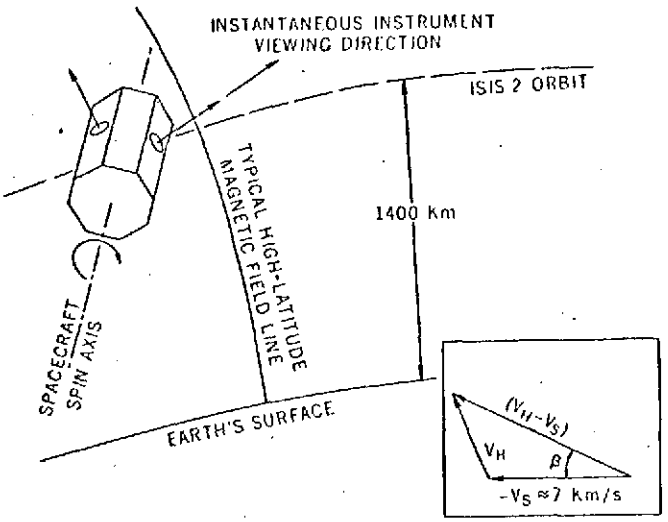

Fig. 1. Diagram of the Isis 2 spacecraft orbital situation for flow observations in the high-latitude region. The insert illustrates the direction of the hydrogen flow vector in the spacecraft reference frame.

consist of a component from spacecraft motion and a component from a flow along the ambient magnetic field in an earth-fixed reference frame. With these assumptions, the H^+ velocity can be computed. For the cases discussed in this work, it is generally in the range 4–10 km/s. This procedure for identification of polar wind light ion flow has been discussed by *Hoffman* [1970].

Given the hydrogen ion mean flow velocity vector as defined by the IMS, and considering the ambient oxygen ions to be corotating with the earth, the RPA data are then used to define the ion energy distribution. We perform a least squares fit to a slightly modified form of the standard [*Whipple*, 1959] RPA response function. In carrying out the summation over the current components due to the three species H^+, He^+, and O^+ the hydrogen and helium are considered to be incident at a velocity V_H and temperature T_H different from the velocity V_o and temperature T_o of the oxygen. Both V_H and V_o are known functions of time as the spacecraft rotates about its spin axis. The two temperatures, the corresponding densities, the 'background' flux of suprathermal electrons, and the spacecraft potential were the parameters to be determined.

Recent work has shown the existence of east-west directed flows of 1–2 km/s at high latitude [e.g., *Cauffman and Gurnett*, 1971; *Heppner et al.*, 1971; *Banks et al.*, 1973]. Since these flows are nearly transverse to the Isis 2 polar orbit, their projection into the orbit plane is nearly zero, and the instruments scanning in the orbit plane to sample vertical flows will not be sensitive to their presence. This result is confirmed by the agreement in time in Figure 2 between the maximums of the oxygen peaks and the maximums of the cosine of the angle between the sensor direction and the spacecraft velocity direction. An additional fact that minimizes the effect of the transverse flows is that their moderate velocity is significantly less than either the spacecraft velocity or the proton flow velocity. A 1-km/s transverse velocity would lead to an error of about 8° in the assumed direction of flow of the ambient ions. This error propagates into the temperature determination for both species approximately as the $\cos^2(8°)$; as a result, there is a negligible change in the inferred temperatures.

An example of RPA data for one of the cases of polar wind observation is shown in Figure 3. The data points shown, constituting one *I-V* curve, were obtained in 1 s. Since only data obtained when the instrument is pointed within about 45° of the flow direction can be used, and since the instrument has several sequential modes of operation, only one or two useful *I-V* curves are obtained during each spin period. The electrostatic retardation of the light ions and thus the observation of their energy distribution occur primarily in the energy range 0–2 eV. The oxygen ions are retarded primarily in the energy range 3–5 eV. In the example shown, there is a significant percentage of light ions present, and a good determination of both of the temperatures can be obtained. There is an experimental difficulty as the percentage of either of the species drops below about 5%. This is illustrated by the solid line in the figure, which is the curve for the oxygen component of the plasma. The contribution of the light ions to the total current is the difference between the total current (dots) and the oxygen component (solid curve). As the percentage of light ions decreases, the two curves approach each other, and their difference is determined less accurately. Ultimately, for a sufficiently small light ion component the one- and two-component response functions fall within the resolution limit of the telemetry system, and separate temperatures cannot be inferred. Thus the two-temperature analysis can only yield meaningful results where at least several percent of the minor constituent is present.

For comparison, a number of cases have been analyzed in which no relative flow of protons was observed. That is, the ambient ions, both H^+ and O^+, were considered to be incident on the spacecraft at the negative of the spacecraft velocity, and they were assumed to be at different temperatures. For these cases, the two species are often in thermal equilibrium, but there are also instances of nonequilibrium. The general problem of differential ion temperatures, or other deviations from thermal equilibrium [e.g., *Cole*, 1971; *Schunk and Walker*, 1972], will be considered separately.

Results and Discussion

Only a small number of spacecraft passes have thus far been identified for which both the angle of flow and the two temperatures can be determined. The results for these passes are listed in Table 1 along with appropriate spacecraft orbital information. One of the passes (2151 on April 27, 1971) is at the plasmapause. All other passes are substantially poleward of the plasmapause in a very broad region of upward light ion

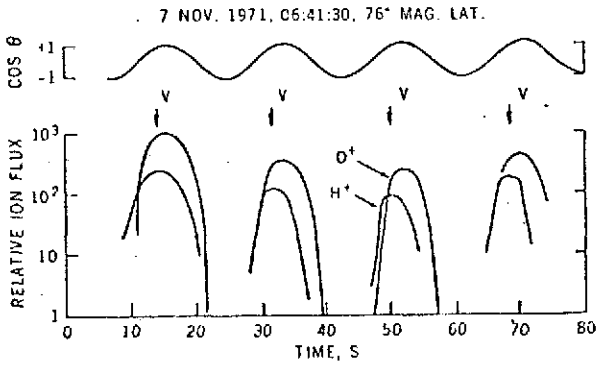

Fig. 2. The IMS O^+ and H^+ response in the ion flow region. The cosine function at the top is of the angle θ between the instrument sensing direction and the spacecraft velocity. The V's, denoting the closest approach to the ram direction, are seen to align well with the maximums of the O^+ flux. The H^+ peaks, beneath the arrows, occur earlier in time than the O^+ peaks; thus a different direction of apparent flow is indicated.

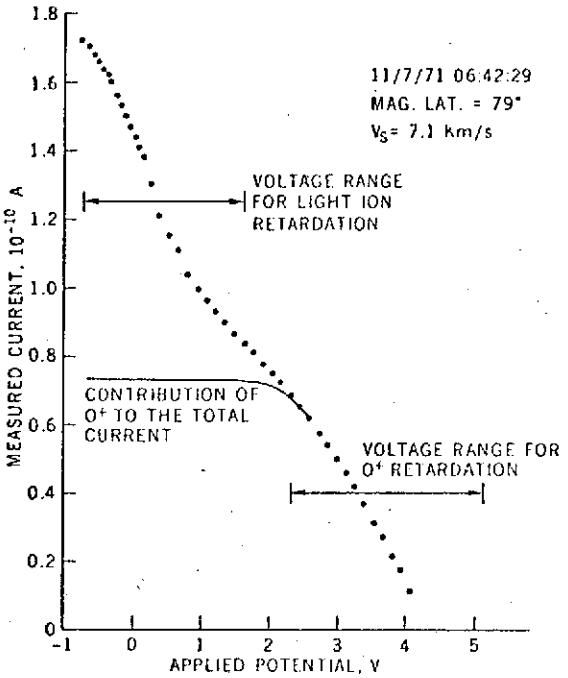

Fig. 3. The RPA integral ion energy spectrum sample illustrating the two regions of the instrument response in which one can obtain good measurements of the energy distributions of the light and heavy ion components of the plasma.

flow. In addition to the temporal and spatial variations present, it is clear that the hydrogen ions are almost always at a significantly higher temperature than the O^+ ions. The ratio of T_H/T_o varies from about unity to almost 10; it is generally in the range from 1.3 to 2.

Banks [1973] has presented a treatment whereby he obtains a limit on the deviation between the temperature of the major constituent and the temperature of the minor constituent in a region where the light minor ion is flowing through a static major ion distribution. He considers the energy balance and finds that, for the idealized case, the 'source' of enhanced energy for the light minor ions is the occurrence of collisions with the major ions through which the H^+ is flowing. These collisions provide a mechanism that couples the flow energy of the H^+ (of order $1/2\ mV_H^2$) to the thermal energy of the H^+ (of order $3/2\ kT_H$).

As a consequence of the low electron to proton mass ratio, the momentum exchange with the ambient electrons (which are as numerous as the O^+ ions) is not significant. The electron energy itself is not increased noticeably, since the electron thermal velocity is much greater than the sum of V_H and the proton thermal velocity. Conversely, the protons are themselves not significantly affected by their collisions with the electrons.

A more complete solution to this problem would involve simultaneous solution of the continuity and momentum equations with the H^+, O^+, and electrons postulated to have different temperatures.

Conclusions

Observations from the Isis 2 spacecraft have established that the hydrogen ions, in the region of polar wind flow, are at a substantially higher temperature than the predominant oxygen ions. These observations were made at an altitude of 1400 km, essentially within the region of transition from a 'collision dominated' to a collisionless medium. The thermal energy enhancement of the hydrogen ions is roughly consistent with a transfer of a significant fraction of their observed bulk flow energy into thermal motion.

It is clear that the general problem of the existence of a nonequilibrium distribution function for the ions is of great significance. The polar wind case discussed here is but one example of the class of problems in which the transition from the 'ionospheric' to the 'plasmaspheric' domain is the significant factor. Other cases, not involving such high-velocity directed flows, will be considered in the future. For example, the ion population in the protonosphere has access, at the apex of the field line, to energization processes that may elevate it to a different temperature from that of either the electrons or the neutral exosphere. The Isis 2 spacecraft, in circular orbit at 1400 km, is at an extremely opportune altitude to carry out studies yielding insight into the rather complex

TABLE 1. Results of the Two-Temperature Analysis for the Cases Identified Thus Far

Time, UT	Flow Angle,* deg	H^+ Velocity, km/s	T_H†	T_o†	$[H^+]$	$[H_e^+]$	$[O^+]$	Latitude, deg	Magnetic Latitude, deg	L	Time, LT
					April 27, 1971						
1423	27	3.7	2319	1836	377		3558	−86.7	−81.1	23.2	1920
1428	27	3.7	3096	1829	890		1306	−77.0	−71.4	11.6	0425
2151	40	10.8	7250	4350	2200	780	2030	−66.5	−55.1	3.2	1712
2151	40	10.8	3882	3075	730	860	1630	−66.5	−55.1	3.2	1712
					October 22, 1971						
0225	39	6.7	2644	1526	31	35	299	70.4	69.3	8.8	0302
0227	39	6.7	9486	1365	53		148	64.5	64.0	5.6	0308
					November 7, 1971						
0641	40	6.2	6090	1399	410		843	87.3	76.7	34.7	1717
0642	40	6.2	8157	847	150	50	170	87.9	79.1	68.4	1912
0644	40	6.2	1255	1337	128	103	501	83.0	85.1	99.0	0108
					November 14, 1971						
0147	35	6.1	3362	1787	225	0	422	61.3	64.3	5.2	0125

* Refers to the spacecraft rotation that occurred between observation of the H^+ flux maximum and the O^+ flux maximum.

† The statistical errors on the temperatures are such that items 2, 4, and 9 may have T_H consistent with T_o. For all the other items, the temperature difference is more than 3 standard deviations.

coupling between the lower atmosphere and the protonosphere.

Acknowledgments. The Editor thanks T. E. Holzer and R. W. Schunk for their assistance in evaluating this paper.

REFERENCES

Banks, P. M., Ion heating in thermal plasma flows, *J. Geophys. Res.*, *78*, 316, 1973.

Banks, P. M., J. R. Doupnik, and S.-I. Akasofu, Electric field observations by incoherent scatter radar in the auroral zone, *J. Geophys. Res.*, *78*, 6607, 1973.

Cauffman, D. P., and D. A. Gurnett, Double-probe measurements of convection electric fields with the Injun 5 satellite, *J. Geophys. Res.*, *76*, 6014, 1971.

Cole, K. D., Atmospheric excitation and ionization by ions in strong auroral and man-made electric fields, *J. Atmos. Terr. Phys.*, *33*, 1241, 1971.

Heppner, J. P., J. D. Stolarik, and E. M. Wescott, Electric field measurements and the identification of currents causing magnetic disturbances in the polar cap, *J. Geophys. Res.*, *76*, 6028, 1971.

Hoffman, J. H., Studies of the composition of the ionosphere with a magnetic deflection mass spectrometer, *Int. J. Mass Spectrom. Ion Phys.*, *4*, 315, 1970.

Schunk, R. W., and J. C. G. Walker, Ion velocity distribution in the auroral ionosphere, *Planet. Space Sci.*, *20*, 2175, 1972.

Whipple, E. C., The ion trap results in 'Exploration of the Upper Atmosphere with the Help of the Third Soviet Sputnik,' *Proc. IEEE*, *47*(H), 2023, 1959.

(Received December 26, 1973;
accepted February 11, 1974.)